# A Review on Aging-Aware System Simulation for Plug-In Hybrids

Tobias Frambach<sup>®</sup>, Ralf Liedtke, Philipp Dechent<sup>®</sup>, Dirk Uwe Sauer<sup>®</sup>, and Egbert Figgemeier<sup>®</sup>

Abstract—The lithium-ion battery is a vital powertrain component in plug-in hybrid electric vehicles (PHEVs). The fuel reduction potential and cost-effectiveness of these vehicles depend on the sizing of the powertrain components and their utilization, which is defined by the energy management system (EMS). The battery is affected by power and capacity reduction over the lifetime of the vehicle, which needs to be considered during the design process to ensure the performance goals throughout the vehicle's lifetime. Current literature regarding battery aging usually contains experimental results, which are not transformed into a useful aging model for system simulations. Consequently, battery aging is often neglected, which is why this article intends to help researchers understand the degradation process of batteries in PHEVs and consider this in their simulation and dimensioning process. First, PHEV powertrain topologies and components are presented. Afterward, battery degradation mechanisms and recent findings are explained, followed by appropriate modeling approaches for different simulation targets. Finally, current aging-aware EMS literature is systematically reviewed, and the integration of the aging models is analyzed, so researchers in system simulation areas can improve their powertrain models.

Index Terms—Battery degradation modeling, energy management strategy (EMS), lithium-ion battery, plug-in hybrid electric vehicle (PHEV).

# I. INTRODUCTION

THE automotive industry is currently facing a change concerning powertrain technology. Shrinking oil reserves [1], climate change, stricter emission regulations, and threats of

Manuscript received March 16, 2021; revised May 28, 2021; accepted July 6, 2021. Date of publication August 11, 2021; date of current version April 20, 2022. (Corresponding author: Egbert Figgemeier.)

Tobias Frambach is with Robert Bosch GmbH, 71701 Schwieberdingen, Germany, and also with the Institute for Power Electronics and Electrical Drives (ISEA), RWTH Aachen University, 52066 Aachen, Germany (e-mail: tobias.frambach@rwth-aachen.de).

Ralf Liedtke is with Robert Bosch GmbH, 71701 Schwieberdingen, Germany (e-mail: ralf.liedtke@de.bosch.com).

Philipp Dechent is with the Institute for Power Electronics and Electrical Drives (ISEA), RWTH Aachen University, 52066 Aachen, Germany, and also with Juelich Aachen Research Alliance, JARA-Energy, 52428 Juelich, Germany (e-mail: philipp.dechent@isea.rwth-aachen.de).

Dirk Uwe Sauer is with the Institute for Power Electronics and Electrical Drives (ISEA), RWTH Aachen University, 52066 Aachen, Germany, also with Juelich Aachen Research Alliance, JARA-Energy, 52428 Juelich, Germany, also with the Institute for Power Generation and Storage Systems (PGS), E.ON ERC, RWTH Aachen University, 52074 Aachen, Germany, and also with the Helmholtz Institute Münster (HI MS), IEK-12, Forschungszentrum Jülich, 48149 Münster, Germany (e-mail: dirkuwe.sauer@isea.rwth-aachen.de).

Egbert Figgemeier is with the Institute for Power Electronics and Electrical Drives (ISEA), RWTH Aachen University, 52066 Aachen, Germany, and also with the Helmholtz Institute Münster (HI MS), IEK-12, Forschungszentrum Jülich, 48149 Münster, Germany (e-mail: e.figgemeier@fz-juelich.de).

Digital Object Identifier 10.1109/TTE.2021.3104105

cities such as London, Paris, and Stuttgart banning vehicles with combustion engines [2] have accelerated the demand for electrified powertrains. Hybrid electric vehicles (HEVs), plug-in HEVs (PHEVs), and electric vehicles (EVs) offer the potential to decarbonize the transportation sector when using it with renewable energy sources due to increasing the share of electric energy used for vehicle propulsion [3], [4].

PHEVs offer great potential to meet the future environmental requirements of the powertrain. Compared to EV systems, PHEVs utilize an additional conventional fuel-based powertrain with an internal combustion engine (ICE). This results in an extended driving range comparable to conventional vehicles, while the electrical system can be designed with a smaller capacity compared to EVs [5]. In contrast to HEVs, the PHEV powertrain includes an external charge-plug for electric energy and larger-sized electric components, allowing a higher share of electric driving and subsequently a lower fuel consumption. In addition to design considerations [6], having two different energy sources on board makes the system more complex, so a robust, optimal, and admissible energy management system (EMS) that can optimize different performance targets is required to control the power flow inside the vehicle [7].

Furthermore, the sizing of the components is essential, so the system is not overdimensioned and uneconomical for the customer. Despite the average-sized components for PHEVs, the battery still accounts for a high share of the powertrain costs [8] and needs to be dimensioned accordingly [9] to grant a total cost of ownership (TCO) benefit [10], [11]. The battery is usually oversized because the battery cells degenerate throughout the lifetime, resulting in a capacity and power fade. To comply with car manufacturers' warranty agreements for the battery lifetime and meet future emission requirements [12], [13], it is crucial to predict the battery degradation precisely and oversize the components as little as possible. In addition, real-world driving emissions [14] and inservice conformity requirements [15] of the powertrain system emphasize the need for a complete lifecycle analysis of all components.

Recently, the combination of EMS with battery aging models has gained a research interest. EMSs are typically designed for minimizing fuel consumption, but additional optimization targets can also be added. Considering battery aging in the EMS can mitigate the capacity and power fade, therefore reducing the size and costs of the overdimensioned battery [16], [17]. The aging-aware PHEV strategy can be

improved by prediction data [18], used for hybrid energy storage systems (HESSs) [19], and include charging influences [20]. A review of general battery aging mechanisms can be found in [21] and [22] and in [23] with a special focus on automotive aspects. Jaguemont *et al.* [24] concentrate on the mechanisms at cold temperatures and thermal management strategies considering these effects. EMSs are reviewed in [25] and [26] for all hybrid vehicles, while a more detailed review for PHEVs can be found in [27] and [28].

The review has been done for battery aging and EMSs separately, but a combination of both perspectives is necessary for a comprehensive and optimal PHEV system optimization. In detail, this means that many aging models are not intended for implementation in an EMS, and studies focusing on improving energy management do not include battery aging in their simulations. This study aims to close the gaps between these two disciplines and give researchers insights into both domains. Therefore, an overview of currently known aging mechanisms and their influencing operating parameters is given. Subsequently, battery aging models, which are widely used in the field of EMS and recent ones, are reviewed. Degradation models adapted to PHEVs are discussed separately with their key differences. Next, we gather aging-aware PHEV studies, categorize them by EMSs types, and discuss their key findings. Finally, open issues and future investigation topics are identified, which can serve as a starting point for researchers.

The remainder of this article is structured as follows. Section II describes the possible PHEV powertrain topologies. After defining the topology, the battery component is analyzed further. Section III presents the aging mechanisms and their origins inside a battery cell. In Section IV, the possible methods to model battery aging are discussed. Section V classifies EMSs and presents published methods, which considers battery aging and fuel consumption for PHEVs. Discussion and future research topics are shown in Section VI. Finally, Section VII summarizes the key findings of this article.

#### II. POWERTRAIN TOPOLOGIES FOR PHEVS

In this section, the basic powertrain topologies for PHEVs are explained. The differentiation is vital for powertrain modeling. Each topology provides individual functions and advantages for specific vehicle operating cases, as shown in Table I. HEVs are operated in charge sustaining mode only, where the battery energy is controlled around a mean value, and only the electric motor provides electric energy during recuperation and load point shifting or rising. PHEVs have an additional onboard charger to use grid electricity. The vehicle can be operated in charge sustaining mode but additionally in a depleting mode with a charged battery, using the grid energy for longer electric driving periods compared to HEVs. More detailed insights can be found in [29], including challenges and subtypes or in [30], where component sizing methods and EMSs are reviewed as well. The topologies can be distinguished into series, parallel, and power-split configurations.

TABLE I
HYBRID VEHICLE FUNCTIONS FOR DIFFERENT TOPOLOGIES

	Series	Para	Power- split				
		P0	P1	P2	P3	P4	
Pure electric driving	✓	-	-	✓	✓	✓	✓
Pure ICE driving	-	✓	✓	✓	✓	✓	✓
Boosting	-	✓	✓	✓	✓	✓	✓
Load point rising	✓	✓	✓	✓	✓	✓	✓
Load point shifting	✓	-	-	-	-	-	✓
Stationary charge mode	✓	✓	✓	✓	-	-	✓
Electric all- wheel drive	-	-	-	-	-	✓	-
Recuperation	✓	✓	✓	✓	✓	✓	✓
PHEV applicable	✓	-	-	✓	✓	✓	✓

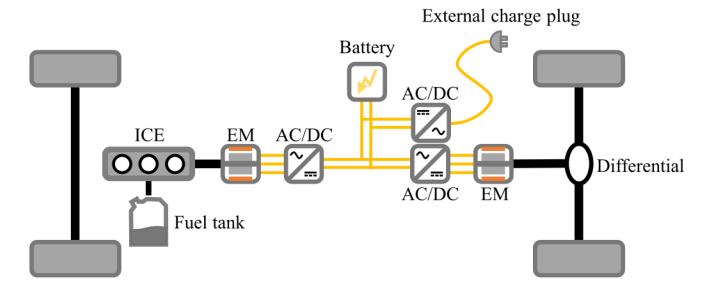


Fig. 1. Series plug-in hybrid topology.

#### A. Series Hybrid Electric Vehicles

The ICE has no direct mechanical connection to the wheels in a series HEV (see Fig. 1), but it is connected in series with a generator and an electrical motor. The ICE powers the generator, which is connected to a battery. The drive axle is only connected to an electrical motor. The ICE can always run in the optimal operating area because it is not coupled to the current power demand. The conversion of the energy twice, once in the generator and second in the electric motor, leads to additional irreversible power losses. Generally, this topology is efficient in dynamic urban driving profiles with high standstill times and many recuperation phases. Therefore, it is often used for buses, construction, and heavy vehicles [27], [31], [32]. An example of the topology commonly available in the passenger car market is the BMW i3, where the range extender version operates as a series PHEV.

#### B. Parallel Hybrid Electric Vehicles

If the ICE and electric motor can propel the vehicle simultaneously, the system is called a parallel HEV (see Fig. 2). A further distinction is usually made for the positioning of the electric motor within the powertrain, referred to as P0–P4 [33]. PHEVs are made to drive in electric mode, which requires at least a P2 system, where the electric motor is

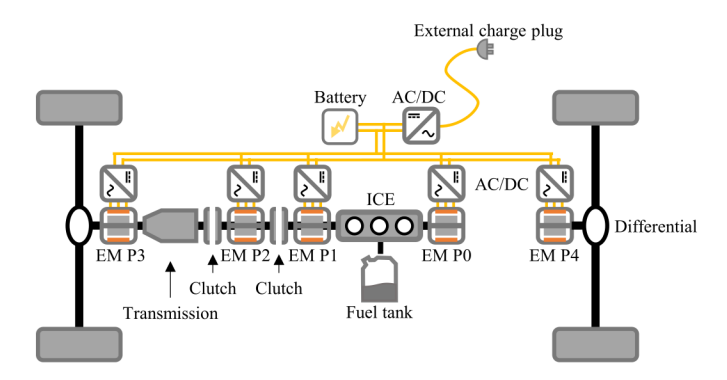


Fig. 2. Parallel plug-in hybrid topology.

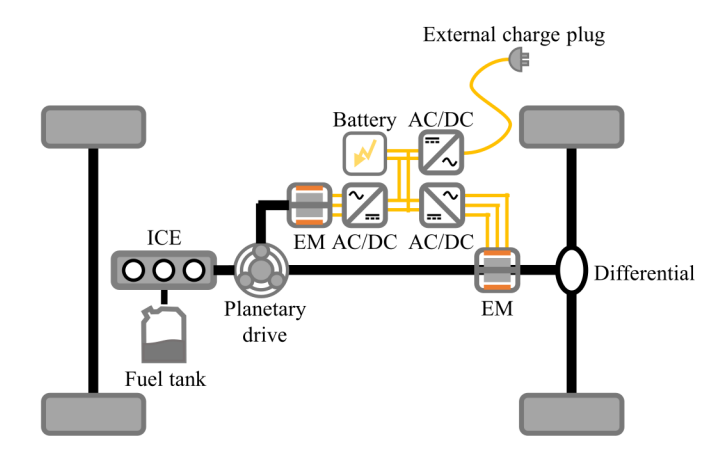


Fig. 3. Power-split plug-in hybrid topology.

placed after the clutch. Parallel systems are more efficient for extra-urban and highway driving profiles [27], [32], [34]. Examples of parallel hybrid vehicles PHEVs on the road are BMW 330e (P2), Volkswagen Passat PHEV (P2), and the Mini Countryman PHEV (P0 + P4).

## C. Power-Split Hybrid Electric Vehicles

A power-split hybrid offers the possibility to split the ICE's input power into a mechanical and an electric path with a planetary gear set (see Fig. 3). These systems require two electric machines and at least one planetary gear, making the powertrain expensive and complex in terms of packaging and the EMS [27], [32], [35]. The Toyota Motor Company is well known for its power-split hybrids, such as the Prius or RAV4, which also offers a PHEV version. Additional to series, parallel, and power-split hybrids, there are mixed forms on the market to combine the advantages. However, the powertrain will become more complex and expensive because additional components and connecting elements are required.

# III. DEGRADATION OF LITHIUM-ION BATTERIES

Every electrified powertrain topology consists of at least one energy storage system. Today's electrified vehicles typically use lithium-ion batteries to store electrical energy due to the high energy density. The lithium-ion cells degrade during

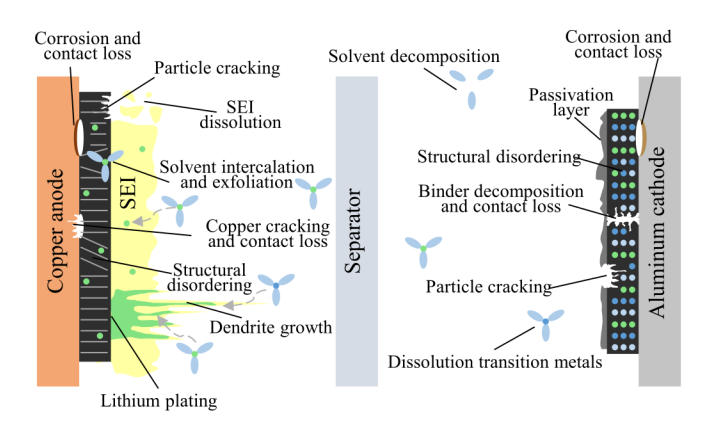


Fig. 4. Aging mechanisms in lithium-ion cells (adapted from [36]).

lifetime operation due to several aging mechanisms, as shown in Fig. 4. These are discussed in the following, including the originating factors. Finally, some recent discoveries regarding reversible effects on aging are shown, which leads to different capacity trends in real-life applications compared to stationary laboratory testing.

### A. Anode

The negative copper electrode is typically coated with graphite, silicon, carbon, or titanate. The most widely used material is graphite because of its balanced characteristics regarding energy and power density over a lifetime [37]. Silicon promises higher gravimetric energy densities; however, it exhibits significant volumetric changes during cycling, resulting in a low lifetime performance because of the mechanical stress in the material. Current research is focusing on increasing the share of silicon in a mixture with graphite further [38], [39].

The primary aging effect for lithium-ion cells with graphite occurs between the electrolyte and coated electrode. The potential of graphite is outside the operating voltage range of the electrolyte [40]. Accordingly, a layer called solid electrolyte interphase (SEI) on the graphite is created with time [41], which prevents further electrolyte degradation from electrons and impedes current collector corrosion [21]. The buildup of this passivation layer leads to a loss of lithium

inventory (LLI). Consequently, the capacity of the battery is reduced, whereas the internal resistance rises due to the resistive film [42]. Even though the layer protects the anode, a further expansion of the SEI is still possible. Graphite exhibits a volume expansion during cycling, which can crack the SEI layer [43], [44]. The SEI can penetrate the electrode and the separator, which can lead to a smaller accessible active surface area [21]. Additional to the SEI growth, the dissolution at higher temperatures of the SEI accelerates the aging process. A decomposition of the protecting SEI layer results in lithium corrosion and lithium salt side products, which are less permeable for ions [45], [46].

Another well-discussed degradation mechanism is reducing lithium ions on the active material in the form of metal lithium. This reaction occurs if the anode potential falls below the standard potential of 0V against Li/Li+, which is enhanced by low temperatures and high charging currents [47], [48]. This can lead to the deposition of metallic lithium called lithium plating, which can be reduced by prohibiting charging at low temperatures in the EMS. The plating process consumes cyclable lithium resulting in a capacity fade. The LLI is accompanied by further electrolyte degradation by reactions with metallic lithium [49].

Further aging mechanisms occurring at the anode side can be due to electrical contact loss [21], current collector corrosion [50], and graphite exfoliation [51].

#### B. Cathode

Cathode materials for automotive applications consist of nickel cobalt aluminum (NCA), nickel cobalt manganese (NMC), lithium manganese oxide (LMO), or lithium iron phosphate (LFP). The main advantage of NCA is the high energy density with a decent lifetime and power characteristic. On the contrary, this chemistry has a low thermal runaway (self-heating after reaching a defined temperature) safety [52]. NMC shares most characteristics, but the safety is increased, which goes along with a smaller energy density. The research focuses on a higher share of nickel for a higher energy density [53]. The lower amount of manganese and cobalt leads to lower cycle life, safety, and conductivity, which has to be managed [54], [55]. LFP profits from the absence of the expensive materials as well [56] and is the safest material regarding thermal runaway among these [57], [58]. In addition, the cycle and calendar life are prolonged [59] even though the iron ions tend to dissolute in the electrolyte as well [60]. The low voltage and high resistance reduce the energy density of

On the cathode side, a surface layer grows over time as well. The electrolyte oxidation occurs at high temperatures and charge voltages above 4.2 V against Li/Li+. The surface thickness is much smaller, but the electrolyte still degrades, and an impedance increase is measurable [62], [63].

A more severe aging mechanism on the cathode side is the dissolution of transition metals, which is also accelerated at high temperatures and a high state of charge (SOC). As stated previously, this effect is a dominating aging mechanism for manganese and iron-based cathode materials. After the

TABLE II
SUMMARY OF AGING ACCELERATING CONDITIONS AND
ASSOCIATED AGING MECHANISMS

Condition	Operation	Main aging mechanism	Effect
High temperature	Storage and cyclization	SEI growth and dissolution, electrolyte decomposition, metal dissolution	Capacity and power fade
Low temperature	Storage and cyclization	Lithium plating	Capacity and power fade
High SOC	Storage and cyclization	SEI growth, graphite exfoliation, electrolyte, binder decomposition	Capacity and power fade
Low SOC	Storage and cyclization	Current collector corrosion	Power fade
High current	Cyclization	SEI growth, graphite exfoliation, cracking, structural disordering	Capacity and power fade
High DOD	Cyclization	Loss of electrical contact, cracking	Capacity and power fade

dissolution in the electrolyte and the according LAM at the cathode, the metal ions can flow to the anode and accelerate the SEI growth, including LLI and resistance increase there [21], [64].

Structural disordering and phase transitions alter the cathode materials negatively. Similar to the anode, the cathode active material undergoes volume changes during cycling, which stresses the particles mechanically. Also, analogical to the anode mechanisms, current collector corrosion and failure of the binder contribute to the aging of the cathode electrode [21].

#### C. Influencing Operating Parameters

The previously mentioned aging mechanisms occur simultaneously and often interfere with each other. In applications, one individual mechanism's contribution is not relevant, so lifetime indicators are generated to define the state of health (SOH) of a battery. The capacity and power fade are the most used indicators since they are relevant for the operation of EVs. A decrease in capacity leads to a lower electric range, which is especially important for EVs. An increase in resistance results in higher thermal losses [65] and a power fade [24] because the cutoff voltages are reached earlier due to the increased voltage drop. Since HEVs use high-power batteries with a small capacity, this effect is essential for this topology [66]. PHEVs compromise between these topologies, so both capacity fade and resistance increase can be significant [61].

The degradation mechanisms affect the aging indicators in two different ways. Calendar aging describes the aging, which the cell experiences during rest periods. It is dependent on temperature and SOC. Cycling aging refers to the aging in operation mode, so the cell is either charged or discharged. In addition to the temperature and SOC, it depends on the depth of discharge (DOD) and current rate. During cyclization, the cells simultaneously endure calendar aging. To distinguish these two aging origins, calendar and cycle tests are necessary. The calendar aging during the cycle test can be calculated and subtracted from the cycle degradation values to model the cell degradation more precisely [67]–[69].

Even though the relationship between the mechanisms is complex and four different aging drivers are identified, some

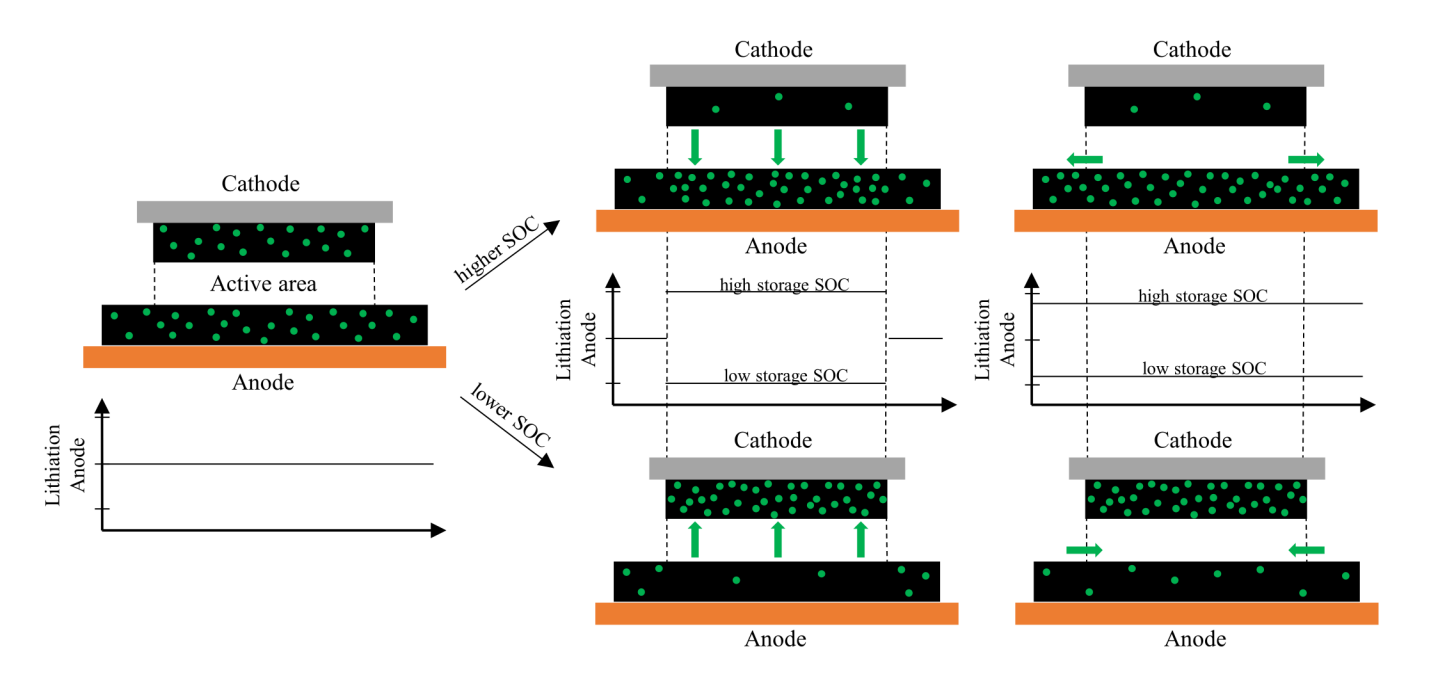


Fig. 5. Qualitative sketch of passive electrode effect for calendar aging, distinguishing between higher (top) and lower (bottom) storage SOC compared to the initial condition (left).

general implications can be given to prolong the battery lifetime (see Table II). High temperatures increase the damaging chemical reaction rate, whereas low temperatures increase lithium plating [24], [70]. The optimal value is dependent on the chemistry and operation profile because the temperature should be low during storage and higher during cycling operation. A tradeoff exists as well for the optimal SOC. Higher SOC levels mainly accelerate SEI growth, whereas low SOC leads to current collector corrosion. The mean SOC during cycling is also important because the same DOD can result in different aging behavior if cycled around different average SOC levels. The current and DOD itself should be low with no phase transitions in-between for a higher battery lifetime [71], [72].

#### D. Reversible Effects

Some studies also mention capacity recovery effects and study the mechanisms behind this phenomenon. The recovery effect can retrieve several percentage points of the nominal capacity, so it has a significant influence on aging experiments' findings. Capacity recovery was reported during storage and during cycling operation, with different possible causal mechanisms. One explanation is called "anode overhang" or "passive electrode effect," which deals with the geometrical oversized anode. The anode in graphite-based cells is dimensioned larger than the cathode to prevent lithium plating. The additional active material, also called overhang, on the anode's edges, does not take part in the intercalation process since the cathode counterpart is missing [73]. This effect is qualitatively explained in Fig. 5. The initial condition is shown on the lefthand side, which occurs after a prolonged storage time with no charging or discharging process. If the SOC of the cell is changed for a consecutive aging experiment, the active areas

change their degree of lithiation due to the charge transfer process. Afterward, lithium ions can diffuse from the active anode part into the overhang or vice versa because of the potential difference between these two regions. The diffusion speed increases with higher temperatures and potential differences between the active and passive areas [74]. During subsequent storage or cycling around the opposite SOC level, the ions move back reversibly to the active part because the driving potential is now reversed [75]. The implications for experiments are essential because the passive electrode effect can make up a difference of several percentage points in capacity and correlates to [76]–[78]

$$Q_{\text{loss,rev}} = (\text{SOC}_{t0} - \text{SOC}_{\text{test}}) \cdot \left(\frac{A_{\text{Anode}}}{A_{\text{Cathode}}} - 100\%\right) \quad (1)$$

where  $SOC_{t0}$  and  $SOC_{test}$  are the initial SOC and storage SOC, respectively.  $A_{Anode}$  and  $A_{Cathode}$  describe the coated areas of the electrodes and lead to a value greater than one. If these results are transferred into an aging model directly, the aging capability is underestimated because cycling in real-life applications with a resulting mean SOC in a medium-range inhibits this process.

#### IV. BATTERY DEGRADATION MODELS

To evaluate the battery aging in a drive cycle simulation or consider it in a vehicle EMS, a control-oriented battery aging model is needed. Several models have been developed over the past, categorized into electrochemical, data-driven, and semiempirical models.

#### A. Electrochemical Models

Electrochemical models simulate the diffusion and charge transfer processes inside a battery cell. With these insights, detailed information about the aging phenomena in the battery cell can be obtained, which allows high-fidelity modeling of the aging phenomena at the electrodes. On the contrary, a high experimental effort and knowledge are required to parameterize the large numbers of variables. Furthermore, the calculation time of electrochemical models is comparably high, which prevents the real-time EMS applicability. Since the SEI growth is the most significant aging mechanism for cells working in the approved operating range, electrochemical aging models focus on generating a health-conscious EMS. In [79], the main equations for the irreversible layer growth on the anode were developed. The growth depending on time and spatial resolution is described by

$$\frac{\partial \delta_{\text{film}}}{\partial t} = \frac{-M_P J_{sd}}{a_n \rho_P F} \tag{2}$$

with the layer's molecular weight  $M_P$ , specific surface area  $a_n$ , mass density  $\rho_P$ , and Faraday's constant F. The local volumetric current density for the side reactions  $J_{sd}$  is given by the Butler–Volmer kinetics.

To make this complex aging model implementable into a real-time control unit, some studies lowered the computational load with approximations and linearization to make them applicable in control-oriented simulations [80]–[84]. Those models are typically used in battery management systems, where real-time measurements are available and the advantages of high model accuracy can be utilized to obtain battery SOH and remaining use of life predictions. Recent literature and reviews exist in this field, and the reader is guided to those [85]–[88].

#### B. Data-Driven Models

These aging models fit a model empirically to a large amount of test data and have gained much interest recently, along with the use of machine learning. After the initial training of the dataset, aging results can be gained very fast without a detailed parameterization or detailed knowledge of the processes inside the cell. However, these models require a large amount of test data and can lead to errors when the cell is operated outside the test range because the model's extrapolation capability is typically weak. An example of an NMC cell study is given in [89] for calendar aging and a separate study for cycle aging [90], where the Gaussian process model can learn and improve itself continuously from real-world operation data. Severson et al. [91] provide a large publically available cycle aging dataset for LFP cells with varying fast charging and constant discharging currents. They use machine learning to predict the cycle life only using voltage curves from early cycles. Further datasets can be found in [92] and [93]. With the use of cloud-connected batteries, more and larger training datasets could be available in the future. Studies already show how the data are transmitted to the cloud and create a digital twin for battery health analysis [94], [95]. Providing the datasets to the public will help in fitting data-driven aging models for system simulations.

#### C. Semiempirical Models

Semiempirical models attempt to combine the advantages of electrochemical and data-driven models and find a compromise between these two. To do this, a mathematical aging model is fit with parameters from experimental results. The function is relatively simple, allowing a fast computation time and implementing the model in a vehicle control unit. Compared to a data-driven model, fewer experiments are necessary, while the semiempirical model can also extrapolate data according to the mathematical function. These characteristics make the semiempirical model very attractive for usage in healthconscious EMS. The challenging task is to find a function that describes the aging behavior well and includes all significant degradation influencing parameters. Therefore, the prediction quality of the models depends on the covered experimental testing points [96]. We focus on studies, which provides data and information to rebuild the aging model and does not require updates over a lifetime with filter algorithms.

1) Cycle Aging: To model the capacity fade in a semiempirical model, physical parameters are considered and fit to predefined equations with the lowest regression error. The equations usually consider the SOC, current, temperature, DOD, time, and energy throughput, given in ampere-hours or cycle numbers.

One of the most widely used aging models that originate from [97] is parameterized for an LFP cell in [98]

$$Q_{\text{loss}} = B \cdot \exp\left(\frac{-E_a}{RT}\right) \cdot Ah^z \tag{3}$$

where B and z are fitting parameters and  $E_a$ , R, T, and Ah describe the activation energy, universal gas constant, temperature, and total Ah-throughput, respectively. The power-law factor z ranges between 0.5 and 1 in most studies. The exponential part of the equation describes Arrhenius-kinetics, which describes the temperature dependence for many chemical reactions and is often applicable to battery aging. In [99], calendar and cycle life are fit with the model from [98] for an NCA cell and a similar LFP cell. In a later study [100], the equation was extended to a control-oriented model including a current and SOC dependence with further experimental calibration

$$Q_{\text{loss}} = (\alpha \cdot \text{SOC} + \beta) \cdot \exp\left(\frac{-E_a + \gamma \cdot I_C}{RT}\right) \cdot Ah^z \quad (4)$$

where  $\alpha$ ,  $\beta$ , and  $\gamma$  are further fitting parameters and  $I_C$  is the current dependence. The literature with cycle life models and the key findings can be found in Table III. Only Hoog *et al.* [68] and Naumann *et al.* [101] include all influencing factors in their experimental design, so the resulting cycle aging models can have a different form, and only a few are validated with a dynamic testing profile. In addition, a comparison between different cell chemistries is impossible, making it challenging to derive a general equation.

2) Calendar Aging: The previously shown aging models concentrate on cycle aging, which is the basis for a controloriented model. For aging-aware sizing of the components, the capacity fade during calendar aging is also essential, as the

TABLE III

CYCLE AGING STUDIES FOR SEMIEMPIRICAL MODELS

Study/ Year	Cell	Investigated factors					Results		Key findings	
1 cai		T	Ah/n	SOC	DOD	$C_{\text{rate}}$	$Q_{loss}$	Rinc		
[102] 2014	Sanyo UR18650W 1.5 Ah Cylindrical NMC+LMO/G	✓	✓		✓	<b>√</b>	✓		<ul> <li>Capacity fade correlates linearly with Ah-throughput</li> <li>T and I more significant than DOD</li> <li>Calendar results included, but from cycle tests with the lowest harm (C/2 and 10% DOD)</li> </ul>	
[68] 2017	EIG 20 Ah Pouch NMC/G	✓	✓	✓	✓	✓	✓		<ul> <li>C-Rate tested but was not significant</li> <li>High DOD and temperatures cause the strongest capacity loss</li> <li>Dynamic validation with driving profile</li> <li>Calendar results included</li> </ul>	
[69] 2014	Sanyo UR18650E 2.05 Ah Cylindrical NMC/G		<b>✓</b>	✓	✓		✓	✓	<ul> <li>Focus on DOD window</li> <li>Capacity fade has square root dependency over Ah-throughput</li> <li>Lowest aging around medium SOC and low DOD</li> <li>Dynamic validation with driving profile</li> <li>Calendar results included</li> </ul>	
[98] 2011	A123 26650 2.2 Ah Cylindrical LFP/G	✓	✓		✓	✓	✓		<ul> <li>DOD tested but was not significant</li> <li>High temperatures and C-Rates cause the strongest capacity fade</li> <li>Charge throughput modeled with power-law factor of 0.55</li> </ul>	
[99] 2016	A123 26650 2.3Ah Cylindrical LFP/G Saft VL6P	<b>✓</b>	✓			✓	✓		<ul> <li>Calendar results collected from [103], cycle aging from [98, 104]</li> <li>Dynamic validation with results from literature for cycle aging</li> <li>Coupling with an electrothermal model for Vehicle-to-Grid studies</li> <li>NCA cell more sensitive to cycle aging than LFP cell</li> </ul>	
	7 Ah Cylindrical NCA/C									
[100] 2016	A123 ANR26650 2.5 Ah Cylindrical LFP/G	✓	✓	✓		✓			<ul> <li>Charge throughput modeled with a power-law factor of 0.57</li> <li>Testing model accuracy with dynamic test from literature</li> <li>Extending the battery aging model with severity factor map for EMS integration</li> </ul>	
[101] 2020	Sony/Murata US26650FTC1 2.85 Ah Cylindrical LFP/G	✓	✓	✓	✓	✓	✓	✓	<ul> <li>Comprehensive cycle aging study, calendar results published in [105]</li> <li>Capacity fade with power-law factor of 0.5, resistance increase with 1</li> <li>Temperature had no significant influence between 25-40°C</li> <li>C-Rate shows minor influence compared to DOD and mean SOC</li> <li>Dynamic validation results included</li> </ul>	
[106] 2015	Unspecified 26650 2.3 Ah Cylindrical LFP/G		✓		✓	✓	✓		<ul> <li>C-Rate effect was minimal, no clear dependency observable</li> <li>Polynomial or exponential influence of DOD depending on the DOD level</li> <li>Dynamic validation results</li> <li>Calendar aging results published in [107]</li> </ul>	
[108, 109] 2020	Kokam SLPB 8043140H5 3.2Ah Pouch NCA+LCO/G	✓	<b>√</b>				✓	✓	<ul> <li>Detailed temperature aging study</li> <li>Internal temperature gradients influence the aging behavior differently compared to steady temperatures</li> <li>Calendar aging results published in [110]</li> </ul>	

allowed capacity fade shrinks during cyclization. Furthermore, it is possible to subtract the capacity loss during the cycle test, which originates from the calendar degradation. Since the cell is not cycled, only the temperature, storage SOC, and time are influencing factors. As a general function, the capacity fade during calendar aging is often stated as

$$Q_{\rm loss} = C \cdot \exp\left(\frac{-E_a}{RT}\right) \cdot t^z \tag{5}$$

where t is the storage time and C a preexponential factor, which can be SOC and temperature-dependent. Published calendar aging studies with model parameters are listed in Table IV. Compared to cycle life models, it can be seen that the calendar aging studies cover all influencing factors more often, and the influences correspond between the different

examinations. Nevertheless, not all studies have a dynamic validation included and consider the anode overhang in their results.

*3) PHEV Adaption:* Some studies also focus on battery aging for PHEV applications. In comparison to the previously stated models, the PHEV models can differ in two ways. First, a detailed investigation of shallow cycling at lower SOC can be done, which corresponds to the charge sustaining operation (see Fig. 6). In this case, the battery has reached the lower SOC limit and is subsequently used as an HEV until it is charged again. In [111], such a model is generated for an LFP cell. The aging model depends on cycle numbers instead of Ah-throughput and is fit according to

$$Q_{\text{loss}} = (\alpha + \beta \cdot \text{DOD} + \gamma * e^{C - \text{Rate}}) \cdot n^{1.36}.$$
 (6)

TABLE IV
CALENDAR AGING STUDIES FOR SEMIEMPIRICAL MODELS

Study/ Cell		Investigated factors			Results		Key findings	
Year		T	SOC	Time	Q <sub>loss</sub>	Rinc		
[102] 2014	Sanyo UR18650W 1.5 Ah Cylindrical NMC+LMO/G	✓		✓	✓		<ul> <li>Data for the calendar aging model originates from cycle tests with the lowest harm (C/2 and 10% DOD)</li> <li>SOC dependency not covered</li> </ul>	
[68] 2017	EIG 20 Ah Pouch NMC/G	✓	✓	✓	✓		<ul> <li>Polynomial fit for capacity loss</li> <li>High temperatures and SOC cause the highest degradation</li> <li>Dynamic validation results</li> </ul>	
[69] 2014	Sanyo UR18650E 2.05 Ah Cylindrical NMC/G	✓	✓	✓	✓	✓	<ul> <li>Time depend with power-law factor of 0.75</li> <li>SOC influence on capacity and resistance is increasing linearly</li> <li>Temperature follows Arrhenius law</li> </ul>	
[99] 2016	A123 26650 2.3Ah Cylindrical LFP/G Saft VL6P 7 Ah Cylindrical NCA/C	✓	✓	✓	✓		<ul> <li>Calendar results collected from [103], cycle aging from [98, 104]</li> <li>SOC dependence of factor B differs for LFP (decreases) and NCA (increases)</li> <li>Power-law factor z is SOC dependent for LFP (decreases), but not for NCA</li> </ul>	
[105] 2018	Sony/Murata US26650FTC1 2.85 Ah Cylindrical LFP/G	<b>√</b>	<b>✓</b>	✓	✓	✓	<ul> <li>Power-law factor 0.5 for capacity fade and 1 for resistance increase</li> <li>Temperature follows Arrhenius law</li> <li>Cubic function for SOC dependence on capacity fade (increasing)</li> <li>Quadratic function for SOC dependence on resistance increase, highest at 50% SOC</li> <li>Anode overhang considered</li> <li>Dynamic validation results</li> </ul>	
[107] 2014	Unspecified 26650 2.3 Ah Cylindrical LFP/G	✓	✓	✓	✓		<ul> <li>Temperature follows Arrhenius law</li> <li>Exponential SOC dependence (increasing)</li> <li>Dynamic validation results</li> </ul>	
[113] 2014	Unspecified 15Ah Cylindrical LFP/G	✓	✓	✓	✓	✓	<ul> <li>Resistance increases linearly with capacity fade</li> <li>SOC shows linear influence, Temperature exponential</li> <li>Dynamic validation results</li> </ul>	
[114] 2012	Unspecified 6Ah unknown NMC/G	✓	✓	✓	✓	✓	<ul> <li>Fitting results for several functions were evaluated</li> <li>Power-law factor 0.5</li> <li>Temperature and SOC accelerate aging exponentially</li> <li>Coupling of impedance model</li> </ul>	
[115] 2013	Unspecified 10Ah Pouch NMC/G	✓	<b>✓</b>	✓	✓	✓	<ul> <li>Open circuit and constant voltage measurements only differ at 100%SOC</li> <li>Power-law factor 0.5</li> <li>Temperature follows Arrhenius law</li> <li>Dynamic validation results</li> </ul>	
[110] 2021	Kokam SLPB 8043140H5 3.2Ah Pouch NCA+LCO/G		✓	✓	✓	✓	<ul> <li>Temperature follows Arrhenius law</li> <li>Proofed that there is no path dependency</li> <li>Fit relies on exponential function</li> </ul>	

Compared to the cycle aging models from Section IV-C1, a linear and exponential dependence of the DOD and current is similar though the power-law factor is above one, which results in faster degradation. The reason for this could be the discharge process until 0% SOC with resulting additional or enhanced aging mechanisms, yet similar results were found in [112]. Shallow cycling around lower SOCs was also considered in [68] and [69].

Second, the aging function can include the time-share spent in charge depleting and charge sustaining mode instead of introducing a separate capacity fade function for the shallow cycling part. The depleting phase is characterized by large pure electric driving distances, which results in higher DODs. A ratio considering this fact is introduced in [116]

$$Ratio = \frac{t_{CD}}{t_{CD} + t_{CS}} \tag{7}$$

with the time spent in charge depleting mode  $t_{\rm CD}$  and charge sustaining mode  $t_{\rm CS}$ . Instead of a constant current discharge process, the cell's power profiles are dynamic and mimic a real-life power consumption in a PHEV. The capacity model for an NMC-LMO cell is stated as

$$Q_{\text{loss}} = (\alpha + \beta \cdot \text{Ratio}^{\gamma} + \delta \cdot (\text{SOC}_{\text{min}} - \text{SOC}_{0})^{\varepsilon}) \cdot \exp\left(\frac{-E_{a}}{RT}\right) \cdot Ah^{z} \quad (8)$$

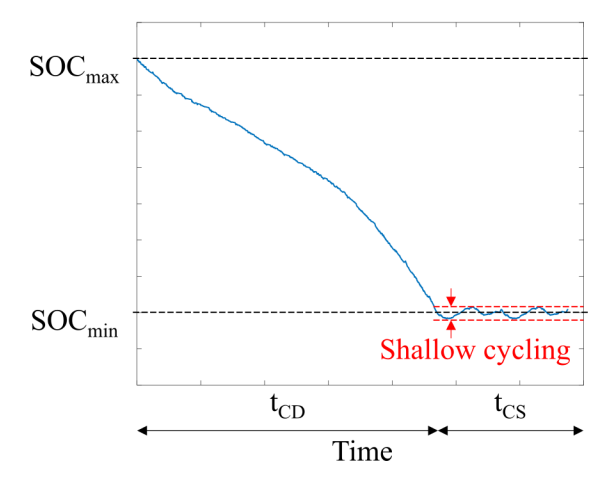


Fig. 6. Share of charge depleting (CD) and charge sustaining (CS).

where  $SOC_0$ ,  $\alpha$ ,  $\beta$ ,  $\gamma$ ,  $\delta$ , and  $\varepsilon$  are fitting parameters and  $SOC_{min}$  is the lower SOC boundary, where the transition to the sustaining mode occurs. The equation agrees with the Arrhenius and power-law function found in other publications. The lowest aging rate can be achieved in charge sustaining mode with a ratio of zero, whereas operation in charge depleting mode leads to the highest capacity face. A resistance model can be found in this article as well, which is also dependent on the charging current rate CR

$$R_{\rm inc} = D({\rm SOC_{min}}, {\rm Ratio}, {\rm CR}) \cdot \exp\left(\frac{-E_a}{RT}\right) \cdot Ah.$$
 (9)

The model was recently used in [117], where a prognostic model predicts the capacity loss and estimates the remaining useful life. A particle filter algorithm estimates the SOC and battery resistance, which serves as an input for a stochastic aging model. This study shows how semiempirical models can serve as online SOH estimators inside battery management systems.

The influence of the ratio is examined further in [118] with LFP cells cycles with a ratio of 0.5 and 0.75. The results show that a larger ratio will accelerate the degradation behavior, but it is important to distinguish between reversible and irreversible capacity loss. About 77% of the capacity loss could be recovered by raising the cutoff voltage, resulting in a remaining capacity fade of only 2% and 4.4%, respectively. Hence, a comprehensive aging model needs to include an evaluation of capacity recovery for PHEV cycling as well.

Similarly, in [119], cells were cycled with a specific PHEV current profile, and the authors investigated the path dependence of power pulses and thermal cycles. Since both influenced the aging behavior, they emphasize the need for more data to predict PHEV aging phenomena realistically.

# D. Summary and Recommendations for PHEV System Simulations

Semiempirical models show the largest potential for integration into control-oriented systems and sizing simulations because they allow a fast and easy prediction of the battery

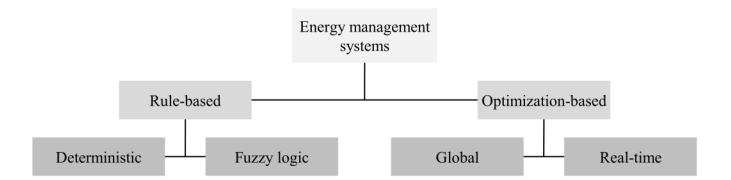


Fig. 7. Categorization of EMSs for aging-aware simulations.

aging despite their nonchemical approach. Only a few studies concentrate on PHEV applications and test appropriate profiles, which differ from HEV and EV profiles due to a mix of charge depleting and charge sustaining cycling. Furthermore, battery cells are customized for HEVs, PHEVs, and EVs, which is roughly expressed in the power-to-energy ratio. Nevertheless, this information cannot be extracted from every paper, making it difficult to find aging models for PHEVs. In addition, the reversible capacity effect is only partly considered, making the model equations questionable. The following aspects should be considered if one published aging model shall be picked or own aging experiments are planned.

- Experiments should contain as many significant factors as possible.
- The factor range should include the typical operation points.
- Calendar aging should be included, especially for sizing studies.
- Systems requiring high power (HEV/PHEV) should also include a resistance model.
- The model and experiments should consider the depleting and sustaining phase.
- 6) The chemistry should match the desired one.
- 7) Commercial cells can show different behavior compared to automotive cells.
- 8) More recent studies, which take state-of-the-art cells into account, are more desirable.

Since it is very challenging to match all of the criteria, further research and publications in this area help to close the gaps and allow higher prediction accuracy.

# V. ENERGY MANAGEMENT STRATEGY CONSIDERING BATTERY DEGRADATION

The EMS target is to split the power in an HEV optimally because the propulsion power can be delivered either by the ICE or by the electric motor. The EMSs can be divided into rule-based (RB) and optimization-based (OB) strategies, as shown in Fig. 7.

## A. Rule-Based Energy Management Strategy

RB strategies divide the power flow according to predefined rules. The simplicity of this EMS allows real-time implementation, therefore usage in vehicle control units. The main difference to OB strategies is the nonoptimality because no optimization process is included in this type of strategy. Tuning of the rules is possible but very time-consuming and dependent on the drive cycle, so optimality cannot be guaranteed for

different driving trips. A further categorization can be done between deterministic and fuzzy logic control strategies.

1) Deterministic Rule-Based Strategy: For deterministic RB strategies, the vehicle operates according to rules so that the main energy sources operate under optimal conditions, e.g., lowest fuel consumption for the ICE or minimal battery degradation for the battery. In [120] and [121], a series PHEV is controlled via two SOC-dependent thresholds, which determines if the required power is delivered by the battery, ICE, or a combination of both. The authors show that the degradation-induced additional energy costs can be reduced with an aging-aware EMS, optimized offline by a particle swarm optimization (PSO). A comparison between RB and OB strategies is done in [17] for a series PHEV bus for optimizing the DOD for minimal operating costs, including equivalent battery degradation costs. The aging models [98], [122] calculate the latter. Despite a comparable low computation time, the results of the OB strategies are better than the RB strategy.

A different RB approach is to distinguish between different frequencies of power demands and split the power accordingly. The ICE encounters difficulties with high-frequency power courses, so it is used for the baseline propulsion power, whereas the electric motor is used for the dynamic peaks. In [123] and [124], a PHEV EMS is investigated with a wavelet transform to decompose the low and high frequencies. The battery degradation could be lowered qualitatively by cutting off the high peak currents of the battery.

2) Fuzzy Logic Rule-Based Strategy: Fuzzy logic-based EMSs are based on qualitative descriptions instead of deterministic rules. The advantages are higher robustness and adaption to different systems compared to deterministic EMS, while it is still easy to implement and real-time capable. A fuzzy-based PHEV with an HESS with a battery lifetime model is optimized in [125]. With the degradation model from [126], it was possible to lower the degradation for several drive cycles. To improve the fuzzy EMS further toward optimality, the rules can be adapted through external optimization algorithms. In [127] the neuro-fuzzy rules are trained with off-line global optimal results considering the TCO, which includes battery aging costs calculated from a DOD-dependent Wöhler curve from [128]. The hierarchical EMS could lower the TCO on vehicle and fleet levels.

#### B. Optimization-Based Strategy

OB strategies can be divided into global and real-time EMSs. The former ones can find the global optimization target but need *a priori* knowledge of the drive cycle or several optimization loops until the optimum is found. In addition, the computation time is extended, which makes vehicle implementation difficult. Real-time EMS overcomes this issue by turning the global cost function into an instantaneous problem, which is solved in every time step. These strategies cannot guarantee a global solution but can produce near-optimal results if the parameters are tuned correctly and robust.

1) Global Optimization-Based Strategy: Despite the computational burden and the real-time inability, the results can serve as a benchmark solution for other strategies and a

template for EMS, which needs to tune rules or parameters. The most discussed strategies are dynamic programming (DP), Pontryagin's minimum principle (PMP), and stochastic search methods (SSMs).

a) Dynamic programming: The DP algorithm divides the drive cycle into discrete time steps. A cost-to-go matrix is built for each time step, which is then solved backward for the path with minimal costs. This approach requires a priori knowledge of the drive cycle, which is why this method is also called deterministic DP (DDP). In [19], the operating costs of a PHEV with an HESS are minimized using the aging model of [98]. The inner loop employs the DP algorithm to minimize battery degradation. The outer loop minimizes the operating costs using simulated annealing (SA), which is an SSM optimization and is explained afterward in this chapter. Compared to a battery pack without ultracapacitors, the costs, battery degradation, and thermal heat dissipation could be decreased. To implement the EMS into a vehicle, the dualloop optimization results are given to a stochastic DP (SDP) algorithm, which is a real-time capable improvement of the DP algorithm. The power demand is considered with a Markov process, which calculates transition probabilities from one state to the next based on several drive cycles. No future driving information is needed because the probabilities only depend on the current Markov state. Still, optimality can only be guaranteed for the drive cycles that are considered in the Markov chain. Moura et al. [129] decrease aging and energy consumption with an SDP algorithm for a PHEV and compare two different aging models. The SEI thickness model from [79] is compared with an Ah-processed model, which minimizes energy throughput. The problem is considered a multiobjective optimization problem with two targets. Since the two targets are conflicting, there is no single but a set of optimal solutions, which are called Pareto-optimal. For these solutions, a single target cannot be improved, without impairing a different target. The Pareto results from randomly generated drive cycles with a Markov chain show different aging models' suggestions. It is beneficial for a low SEI thickness to discharge the battery quickly and avoid high SOC levels. On the contrary, for low energy costs, the battery is depleted slowly to avoid the fuel expensive charge-sustaining mode. The Ah-processed model leads to different results because it will avoid using electrical energy and utilize the ICE in more operating points.

b) Pontryagin's minimum principle: Another global optimization algorithm, the PMP algorithm, reduces the global optimization problem to a local Hamiltonian minimization problem. It delivers only necessary but not sufficient solutions for the global optimum. In return, it has only one tunable parameter and has lower computational requirements than DP. The parameter, also called costate, significantly influences the battery's depleting behavior and needs to be adjusted specifically for every drive cycle. In [130], a charging strategy optimization for PHEVs and BEVs is applied with a semiempirical model from [98] and experimental calibration from [100]. For the optimal control problem and PMP algorithm, a severity factor based on the current, SOC, and temperature is utilized. With the optimal charging profile,

the degradation could be reduced compared to the standard CC-CV profile. In addition, the authors show with a detailed weather and cabin temperature model that solar heat has a significant influence on the severity factor and aging behavior. With the knowledge of environmental data, the charging period could be shifted to an optimal time, where the predicted aging is the lowest. The optimal depleting strategy with PMP is investigated in [131] for a series—parallel PHEV bus with an HESS. The degradation model from [98] is taken, but it is calibrated with the experimental results from [132]. The optimization target was set to minimize the total costs, including equivalent costs for the battery's aging. Compared to a PHEV with only a single battery, the costs could be decreased with an HESS powertrain, mainly due to the lower aging costs.

c) Stochastic search methods: The SSM methods belong to the gradient-free optimization techniques and gain a lot of research interest because of their robustness and global optimum convergence. Typically used SSM algorithms are genetic algorithm (GA), PSO, and SA. A PHEV with a simple RB strategy is optimized in [133]. The rule parameters are improved with a GA in terms of lower fuel consumption and battery degradation. The aging model originates from [116], which also takes the time ratio for charge depleting and sustaining into account. A drive cycle recognition is applied afterward for better adaptability to different driving cycles than the one used in the optimization. With the help of drive cycle recognition, the fuel consumption could be lowered, while the battery degradation also drops slightly. Wang et al. [134] combine SDP with a PSO algorithm to optimize fuel consumption and battery aging for a power-split PHEV simultaneously. They use the severity factor from [135] to calculate the effective Ah-throughput and calibrate it with data from [136] and [137]. The cost function combines two optimization targets by assigning an individual weight to them. The drive cycle is divided into eight segments, where the SDP optimizes the control in each segment. The PSO is used to find a balanced weight factor for each segment with the best tradeoff between fuel consumption and battery aging. In [138], the SEI thickness model from [79] is applied with model order reductions and calculation time improvements presented in [84]. The study deals with a charge pattern optimization for the least costs and battery degradation with changing electricity prices during the day. A nondominating sorting GA determines the Pareto front between the two objectives. The daily driving cycle consists of two driving periods: one in the morning and one in the afternoon. For the lowest battery degradation, no charge is added and the vehicle functions in charge sustaining mode the whole time. The lowest energy costs are achieved when the battery is charged entirely for both trips. To obtain a costefficient charging pattern with low battery aging, the authors suggest charging the vehicle at off-peak hours shortly before the trip.

2) Real-Time Optimization-Based: For an application in a vehicle control unit, the optimization algorithm needs to be calculated in real time. Therefore, the global problem is converted to an instantaneous one to cope with the limited computational power and memory space. These EMS types also

do not require *a priori* drive cycle information because these data are not available in the vehicle. However, some strategies predict future operating points based on the navigation system and sensors (e.g., GPS-sensor). The most discussed real-time OB strategies are the equivalent consumption minimization strategy (ECMS) and the model predictive control (MPC), which can also be extended with prediction data.

a) Equivalent consumption minimization strategy: The ECMS defines a local optimization problem by minimizing the combined fuel consumption from the ICE and the battery's electric energy consumption. To compare the different types of energy sources, an equivalence factor (EF) is assigned to the electric energy. This factor is similar to the costate from the PMP and is significant regarding the performance of the EMS. Because of the significant importance of temperature on battery aging in [139] additional to the fuel consumption minimization, a second constraint on the battery temperature is applied. The thermal constraint is activated if the battery is outside the defined slow-aging temperature zone. For cold temperatures, the battery is heated up quickly at the beginning of the trip, whereas the battery is used less at high ambient temperatures. Both of these characteristics lead to higher fuel consumption and a tradeoff against battery aging. In [140], six different power-split configurations for a PHEV bus are simulated for the lowest fuel consumption and battery degradation. The aging model is adapted from [98] with experimental calibration from [132], [141], and [142]. The comparison between the different configurations reveals that one is superior in terms of aging and fuel economy.

An example of an SOC-adaptive ECMS (A-ECMS) implementation is given in [143] for a PO/P2 PHEV. A PI-controller adjusts the EF during operation. In this study, an electrochemical aging model from [144] is used, and an additional term for aging is added to the cost function. This term assigns high costs for high SOC and current rates because of the increased SEI layer growth. The EMS avoids a long operation time in the high SOC area, large charge currents, and battery utilization. With the adaptive ECMS, battery degradation could be decreased, while the fuel consumption rises only slightly. Another approach with an A-ECMS is recently studied in [145], while this strategy is combined with a neural network and off-line optimizations. The PHEV is modeled with the severity factor aging model from [135] and [146] with the fitting procedure according to [134]. The objective function contains a weight factor for the two conflicting targets, fuel consumption, and battery degradation. As shown in previous studies, a sweep in the weight factor leads to a Pareto front. The controller tries to regulate the SOC to a reference SOC with minimal deviations. In this case, the reference is delivered by a recurrent neural network, which is previously trained offline. Again, the historical dataset is used together with DP to obtain the optimal SOC trajectory. With the adaptive EF, weight factor, and reference SOC, the controller is able to reduce the battery degradation and fuel consumption compared to a simple charge-depleting charge-sustaining strategy, where the battery is depleted much faster. Compared to an SDP-PSO strategy, the equivalent fuel consumption could be decreased with a further fuel save and slight degradation increase. In [147], the ECMS equation is extended with a second state variable for battery degradation. The weight factor between battery aging and fuel consumption is calculated offline with a PMP algorithm. The authors consider calendar aging as well and emphasize that it should be considered for correct TCO calculations with additional aging experiments for the desired onboard battery type. Small differences between the global optimal PMP and proposed dual A-ECMS show improvements for the battery lifetime and fuel consumption at the same time

b) Model predictive control: The algorithm is comparable to DP, but, instead of an infinite time horizon, the MPC optimizes a finite receding horizon. This kind of EMS requires drive cycle prediction or recognition information to optimize a future time window. The data can be gathered by the vehicle navigation system and sensors or by a mathematical model. A series PHEV in charge-sustaining mode controlled by an MPC is studied in [148]–[150] with the aging model from [98]. The sensitivity results highlight the tradeoff between accuracy and calculation time of different battery model fidelities for different objectives [149] and the need for a suitable vehicle mass approximation by the controller [148]. The Pareto front in [150] demonstrates that the MPC controller can reduce the battery aging by almost one-half while keeping the fuel consumption on the same level as an RB thermostat EMS. The study [18] investigates a PHEV bus with different prediction horizon windows and compares the results and the calculation time of an MPC to an RB, DP, and PMP strategy. The degradation is calculated with the severity factor method [146] and the calibration from [100] and [122]. The total cost could be reduced with a health-aware MPC because the savings from a lower battery degradation were higher than the costs for additional fuel. The MPC results lower the costs compared to an RB strategy and come close to the global optimal results from DP or PMP. The cycle calculation time increases with a higher prediction horizon because the DP optimization time is longer. However, even with a 15-s horizon, the model with the lowest total costs, a real-time implementation is possible. In [151], the MPC is combined with an iterative learning control, which improves the optimization target based on historical data and the repetitiveness of power demand when driving fixed routes. The aging model from [100] is taken to optimize the degradation along with fuel consumption. After several iterations, the improved MPC algorithm could get close to the optimal DP results and improved both optimization targets compared to an RB strategy. Similarly, in [152], the MPC optimizes the energy consumption and battery degradation according to [100], while it follows an SOC reference curve generated from a Q-learning algorithm at the vehicle departure. Guo et al. [153] combine the MPC algorithm with the aging model from [98] and reduce it to be only current-dependent. The velocity prediction from a neural network is the basis for the SOC prediction. With this, a cost minimization, including a term for battery aging, is done in the MPC controller, which shows similar results to DP, but is far superior to a simple rule-based strategy. A summary of the presented EMS types can be found in Table V.

TABLE V

EMS Types and Their Characteristics [25], [26]

EMS type	Strategy	Advantages	Disadvantages
Rule-based	Deterministic	<ul><li>Simple and efficient</li><li>Widely used in vehicles</li></ul>	- Calibration effort - No optimality
	Fuzzy logic	<ul><li>Robustness</li><li>Easy to implement</li></ul>	<ul><li>Calibration effort</li><li>No optimality</li></ul>
Optimization- based	DP	<ul><li>Global optimum</li><li>Benchmark solution</li></ul>	<ul><li>A priori drive cycle information</li><li>Computational costs</li></ul>
	PMP	- Global optimal trajectory	<ul><li>A priori drive cycle information</li><li>Computational costs</li></ul>
	SSM	- Non local optimal results	- Parametrization of optimization algorithm
	ECMS	<ul><li>Near optimal results</li><li>Online implementable</li></ul>	- Optimum is drive cycle dependent
	MPC	<ul> <li>Predictive behavior</li> <li>Near optimal results</li> <li>Online implementable</li> </ul>	- Prediction data required

#### VI. DISCUSSION AND FUTURE TRENDS

Battery degradation will have an essential role in the future because overdimensioning the battery pack or not meeting the lifetime requirements will lead to high component costs. Higher degrees of electrification result in increasing battery pack capacities, which will raise the electrical system's cost-share inside a PHEV powertrain further, making it one of the most important parts inside a vehicle. A lack of comprehensive, state-of-the-art, control-oriented battery aging models for PHEVs was identified and requires further exploration. The effects on aging-aware EMSs for PHEVs and optimization frameworks are still not understood completely and can be improved with respect to the optimization, prediction, and coverage of all real-world PHEV operating cases. The remaining challenges and possible starting points for researchers of these topics are summarized in this section.

## A. Battery Aging Models for PHEVs

Over the past years, several aging models for different purposes were published. Semiempirical models gained the most interest in the field of aging-aware EMSs because they offer a compromise between calculation time, experimental effort, and accuracy. However, it was shown that the models still differ from each other, even for the same chemistry. Up until now, no standardized testing procedure and matrix exists, which covers all the degradation-influencing factors. Especially for cycle aging models, it can be seen that some studies contain parameters, which are not present in other models. Only a few experiments cover cycling in charge sustaining and in charge depleting mode. For PHEV powertrain simulations, it is necessary to cover both modes in cycle experiments because the

degradation differs significantly. Shallow cycling around lower SOCs and cycling with high DODs should, therefore, be covered in future publications. For a comprehensive description of battery aging in vehicles, more experiments covering the broad range of chemistries and operating conditions are necessary. In addition, it should be noticed that some studies contain commercial battery cells, which can have a significantly different aging behavior compared to cells certified for automotive usage. More publically available datasets of state-of-the-art battery cells would increase the model quality, especially if the intended application is mentioned for HEVs, PHEVs, and EVs cells. Finally, it is conspicuous that most aging-oriented EMSs use the aging model [98] for a commercial LFP cell. After the publication of this study, further models for automotive applications, including capacity-recovering effects and calendric aging test points, were proposed. Integrating these models could further improve the outcome of EMS optimizations.

#### B. Real-Drive Condition Focus

Additional to the powertrain layout and EMS, the fuel consumption and degradation of the battery are influenced by further boundary conditions, such as the driving profile, charging behavior, and climate conditions [154]. Optimizing PHEV vehicles based on standard driving cycles makes the results comparable, yet the real-world driving energy demand is typically higher. Stochastic models or representative driving cycles would improve the accuracy of studies. In particular, the optimization results for PHEVs depend on the charging behavior as well [20] not only because the charging procedure harms the battery but it will also determine how often the vehicle is driven in charge sustaining and charge depleting mode. Statistical, descriptive models for the charging behavior of the customers are still needed. Finally, extreme temperatures can enhance the auxiliary power demand due to cooling or heating elements, limit the allowed battery power limits, accelerate the degradation mechanisms, and decrease the accessible energy or power inside the battery cells [24], [112]. Publishing models in this area and investigating the influence on battery aging will move the optimization results toward real-life global optimality.

#### C. Comprehensive Optimization Frameworks

Papers discussing aging-aware EMSs and component sizing [19], [155] prove that both domains have to be optimized at the same time because they affect each other. This bilevel optimization procedure leads to a high number of possible combinations, which enlarges even further if two types of energy storage devices are used like in HESSs. This will typically result in large computation times, underlining the need for faster and global optimal optimization methods. Finally, the optimization targets usually focus on fuel consumption, battery aging, or TCO minimization, but further aspects, such as drivability, emissions, and comfort, should be studied additionally.

#### VII. CONCLUSION

This article has reviewed and analyzed the current research status of EMSs considering battery aging, with a special focus on PHEV applications. First, the hybrid powertrain designs are discussed and compared. Next, the main aging mechanisms with their drivers are reviewed, and insight into reversible capacity losses is given. Currently existing aging models used for powertrain simulations and newer ones are summarized, and the special requirements for PHEV applications are explained. The models' divergence showed that more experiments are required to thoroughly understand the degradation and build precise, simple, control-oriented models, especially with PHEV operating conditions. The analysis of current EMSs frameworks revealed that most strategies rely on a few aging models, which does not include experimental findings of recent battery aging research and are not suitable for automotive PHEV applications. Several open issues and starting points for researchers are presented finally. Precise and efficient aging models covering a broad range of operation points for several automotive battery types in combination with real-drive EMSs and sizing optimizations will help to meet PHEVs' lifetime and emission requirements efficiently in the

#### REFERENCES

- N. A. Owen, O. R. Inderwildi, and D. A. King, "The status of conventional world oil reserves—Hype or cause for concern?" *Energy Policy*, vol. 38, no. 8, pp. 4743–4749, Aug. 2010.
- [2] M. Möhner, "Driving ban for diesel-powered vehicles in major cities: An appropriate penalty for exceeding the limit value for nitrogen dioxide?" *Int. Arch. Occupational Environ. Health*, vol. 91, no. 4, pp. 373–376, May 2018.
- [3] S. Ramachandran and U. Stimming, "Well to wheel analysis of low carbon alternatives for road traffic," *Energy Environ. Sci.*, vol. 8, no. 11, pp. 3313–3324, 2015.
- [4] B. Bilgin et al., "Making the case for electrified transportation," IEEE Trans. Transport. Electrific., vol. 1, no. 1, pp. 4–17, Jun. 2015.
- [5] M. Broussely, "Battery requirements for HEVs, PHEVs, and EVs," Electr. Hybrid Vehicles, pp. 305–347, Jul. 2010.
- [6] S. Amjad, S. Neelakrishnan, and R. Rudramoorthy, "Review of design considerations and technological challenges for successful development and deployment of plug-in hybrid electric vehicles," *Renew. Sustain. Energy Rev.*, vol. 14, no. 3, pp. 1104–1110, Apr. 2010.
- [7] S. F. D. Silva, J. J. Eckert, F. L. Silva, L. C. A. Silva, and F. G. Dedini, "Multi-objective optimization design and control of plug-in hybrid electric vehicle powertrain for minimization of energy consumption, exhaust emissions and battery degradation," *Energy Convers. Manage.*, vol. 234, Apr. 2021, Art. no. 113909.
- [8] K. Hamza, K. P. Laberteaux, and K.-C. Chu, "On modeling the cost of ownership of plug-in vehicles," World Electr. Vehicle J., vol. 12, no. 1, p. 39, Mar. 2021.
- [9] Y. Xia, J. Yang, F. Wang, and Q. Cheng, "Impact of battery size and energy cost on the market acceptance of blended plug-in hybrid electric vehicles," *Proc. Comput. Sci.*, vol. 131, pp. 377–386, Jan. 2018.
- [10] C. Hou, H. Wang, and M. Ouyang, "Battery sizing for plug-in hybrid electric vehicles in Beijing: A TCO model based analysis," *Energies*, vol. 7, no. 8, pp. 5374–5399, Aug. 2014.
- [11] D. P. H. Kolodziejak, T. H. Pham, T. Hofman, and S. Wilkins, "An optimization and analysis framework for TCO minimization of plugin hybrid heavy-duty electric vehicles," *IFAC-PapersOnLine*, vol. 52, no. 5, pp. 484–491, 2019.
- [12] J. Zhang, J.-M. Richter, and C. Kaczmarek, "Catalysts for post euro 6 plug-in hybrid electric vehicles," SAE Int., pp. 1–13, Apr. 2020.
- [13] G. Eifler, A. Dau, and M. Wetscher, "Are hybrid-powertrains the right solutions to meet the EU-emission-targets 2030?" in *Proc. Int.* Stuttgarter Symp., 2020, pp. 29–51.

- [14] S. I. Ehrenberger, M. Konrad, and F. Philipps, "Pollutant emissions analysis of three plug-in hybrid electric vehicles using different modes of operation and driving conditions," *Atmos. Environ.*, vol. 234, Aug. 2020, Art. no. 117612.
- [15] Official Journal of the European Union, Commission Regulation-C (2018)6984/969998, Amending Directive 2007/46/EC, Commission Regulation (EC) No 692/2008 and Commission Regulation (EU) 2017/1151, Eur. Union, Brussels, Belgium, 2018.
- [16] S. Xie, X. Hu, Q. Zhang, X. Lin, B. Mu, and H. Ji, "Aging-aware co-optimization of battery size, depth of discharge, and energy management for plug-in hybrid electric vehicles," *J. Power Sources*, vol. 450, Feb. 2020, Art. no. 227638.
- [17] S. Xie, S. Qi, and K. Lang, "A data-driven power management strategy for plug-in hybrid electric vehicles including optimal battery depth of discharging," *IEEE Trans. Ind. Informat.*, vol. 16, no. 5, pp. 3387–3396, May 2020.
- [18] S. B. Xie et al., "Model predictive energy management for plug-in hybrid electric vehicles considering optimal battery depth of discharge," Energy, vol. 173, pp. 667–678, Apr. 2019.
- [19] X. Lu and H. Wang, "Optimal sizing and energy management for cost-effective PEV hybrid energy storage systems," *IEEE Trans. Ind. Informat.*, vol. 16, no. 5, pp. 3407–3416, May 2020.
- [20] X. Hu, C. M. Martinez, and Y. Yang, "Charging, power management, and battery degradation mitigation in plug-in hybrid electric vehicles: A unified cost-optimal approach," *Mech. Syst. Signal Process.*, vol. 87, pp. 4–16, Mar. 2017.
- [21] J. Vetter et al., "Ageing mechanisms in lithium-ion batteries," J. Power Sources, vol. 147, nos. 1–2, pp. 269–281, 2005.
- [22] M. R. Palacín and A. de Guibert, "Why do batteries fail?" Science, vol. 351, pp. 574–581, Feb. 2016.
- [23] A. Barré, B. Deguilhem, S. Grolleau, M. Gérard, F. Suard, and D. Riu, "A review on lithium-ion battery ageing mechanisms and estimations for automotive applications," *J. Power Sources*, vol. 241, pp. 680–689, Nov. 2013.
- [24] J. Jaguemont, L. Boulon, and Y. Dubé, "A comprehensive review of lithium-ion batteries used in hybrid and electric vehicles at cold temperatures," *Appl. Energy*, vol. 164, pp. 99–114, Feb. 2016.
- [25] D.-D. Tran, M. Vafaeipour, M. El Baghdadi, R. Barrero, J. van Mierlo, and O. Hegazy, "Thorough state-of-the-art analysis of electric and hybrid vehicle powertrains: Topologies and integrated energy management strategies," *Renew. Sustain. Energy Rev.*, vol. 119, Mar. 2020, Art. no. 109596.
- [26] P. Zhang, F. Yan, and C. Du, "A comprehensive analysis of energy management strategies for hybrid electric vehicles based on bibliometrics," *Renew. Sustain. Energy Rev.*, vol. 48, pp. 88–104, Aug. 2015.
- [27] M. F. M. Sabri, K. A. Danapalasingam, and M. F. Rahmat, "A review on hybrid electric vehicles architecture and energy management strategies," *Renew. Sustain. Energy Rev.*, vol. 53, pp. 1433–1442, Jan. 2016.
- [28] S. G. Wirasingha and A. Emadi, "Classification and review of control strategies for plug-in hybrid electric vehicles," *IEEE Trans. Veh. Technol.*, vol. 60, no. 1, pp. 111–122, Jan. 2011.
- [29] W. Zhuang et al., "A survey of powertrain configuration studies on hybrid electric vehicles," Appl. Energy, vol. 262, Mar. 2020, Art. no. 114553.
- [30] X. Hu, J. Han, X. Tang, and X. Lin, "Powertrain design and control in electrified vehicles: A critical review," *IEEE Trans. Transport. Electrific.*, vol. 7, no. 3, pp. 1990–2009, Feb. 2021.
- [31] J. van Mierlo and O. Hegazy, "Series hybrid electric vehicles (SHEVs)," Encyclopedia Automot. Eng., pp. 1–12, Apr. 2014.
- [32] M. Ehsani, Y. Gao, and J. M. Miller, "Hybrid electric vehicles: Architecture and motor drives," *Proc. IEEE*, vol. 95, no. 4, pp. 719–728, Apr. 2007.
- [33] Y. Yang, X. Hu, H. Pei, and Z. Peng, "Comparison of power-split and parallel hybrid powertrain architectures with a single electric machine: Dynamic programming approach," *Appl. Energy*, vol. 168, pp. 683–690, Apr. 2016.
- [34] J. van Mierlo and O. Hegazy, "Parallel hybrid electric vehicles (parallel HEVs)," Encyclopedia Automot. Eng., pp. 1–10, Apr. 2014.
- [35] J. van Mierlo, O. Hegazy, J. Smekens, and C. de Cauwer, "Series-parallel hybrid electric vehicles," *Encyclopedia Automot. Eng.*, pp. 1–17, Apr. 2014.
- [36] C. Schlasza, P. Ostertag, D. Chrenko, R. Kriesten, and D. Bouquain, "Review on the aging mechanisms in Li-ion batteries for electric vehicles based on the FMEA method," in *Proc. IEEE Transp. Electrific.* Conf. Expo (ITEC), Jun. 2014, pp. 1–6.

- [37] Y. P. Wu, E. Rahm, and R. Holze, "Carbon anode materials for lithium ion batteries," *J. Power Sources*, vol. 114, no. 2, pp. 228–236, 2003.
- [38] P. Li et al., "Recent progress on silicon-based anode materials for practical lithium-ion battery applications," *Energy Storage Mater.*, vol. 15, pp. 422–446, Nov. 2018.
- [39] M. Salah, P. Murphy, C. Hall, C. Francis, R. Kerr, and M. Fabretto, "Pure silicon thin-film anodes for lithium-ion batteries: A review," *J. Power Sources*, vol. 414, pp. 48–67, Feb. 2019.
- [40] X. Han, M. Ouyang, L. Lu, J. Li, Y. Zheng, and Z. Li, "A comparative study of commercial lithium ion battery cycle life in electrical vehicle: Aging mechanism identification," *J. Power Sources*, vol. 251, pp. 38–54, Apr. 2014.
- [41] E. Peled and S. Menkin, "Review—SEI: Past, present and future," J. Electrochem. Soc., vol. 164, no. 7, pp. A1703–A1719, 2017.
- [42] J. Christensen and J. Newman, "Effect of anode film resistance on the charge/discharge capacity of a lithium-ion battery," *J. Electrochem.* Soc., vol. 150, no. 11, p. A1416, 2003.
- [43] N. Lin et al., "Understanding the crack formation of graphite particles in cycled commercial lithium-ion batteries by focused ion beam–scanning electron microscopy," J. Power Sources, vol. 365, pp. 235–239, Oct. 2017.
- [44] H. Zheng et al., "Correlation between lithium deposition on graphite electrode and the capacity loss for LiFePO<sub>4</sub>/graphite cells," *Electrochim. Acta*, vol. 173, pp. 323–330, Aug. 2015.
- [45] M. Broussely et al., "Main aging mechanisms in Li-ion batteries," J. Power Sources, vol. 146, nos. 1–2, pp. 90–96, 2005.
- [46] V. A. Agubra and J. W. Fergus, "The formation and stability of the solid electrolyte interface on the graphite anode," *J. Power Sources*, vol. 268, pp. 153–162, Dec. 2014.
- [47] N. Legrand, B. Knosp, P. Desprez, F. Lapicque, and S. Raël, "Physical characterization of the charging process of a Li-ion battery and prediction of Li plating by electrochemical modelling," *J. Power Sources*, vol. 245, pp. 208–216, Jan. 2014.
- [48] M. Ecker, P. S. Sabet, and D. U. Sauer, "Influence of operational condition on lithium plating for commercial lithium-ion batteries electrochemical experiments and post-mortem-analysis," *Appl. Energy*, vol. 206, pp. 934–946, Nov. 2017.
- [49] M. Petzl, M. Kasper, and M. A. Danzer, "Lithium plating in a commercial lithium-ion battery—A low-temperature aging study," *J. Power Sources*, vol. 275, pp. 799–807, Feb. 2015.
- [50] C. Fear, D. Juarez-Robles, J. A. Jeevarajan, and P. P. Mukherjee, "Elucidating copper dissolution phenomenon in Li-ion cells under overdischarge extremes," *J. Electrochem. Soc.*, vol. 165, no. 9, pp. A1639–A1647, 2018.
- [51] G.-C. Chung, H.-J. Kim, S.-I. Yu, S.-H. Jun, J.-W. Choi, and M.-H. Kim, "Origin of graphite exfoliation—An investigation of the important role of solvent cointercalation," *J. Electrochem. Soc.*, vol. 12, no. 147, pp. 4391–4398, 2000.
- [52] A. W. Thompson, "Economic implications of lithium ion battery degradation for vehicle-to-grid (V2X) services," *J. Power Sources*, vol. 396, pp. 691–709, Aug. 2018.
- [53] S.-T. Myung et al., "Nickel-rich layered cathode materials for automotive lithium-ion batteries: Achievements and perspectives," ACS Energy Lett., vol. 2, no. 1, pp. 196–223, Jan. 2017.
- [54] H.-J. Noh, S. Youn, C. S. Yoon, and Y.-K. Sun, "Comparison of the structural and electrochemical properties of layered Li[Ni<sub>x</sub>Co<sub>y</sub>Mn<sub>z</sub>]O<sub>2</sub> (x = 1/3, 0.5, 0.6, 0.7, 0.8 and 0.85) cathode material for lithium-ion batteries," *J. Power Sources*, vol. 233, pp. 121–130, Jul. 2013.
- [55] M. Li and J. Lu, "Cobalt in lithium-ion batteries," Science, vol. 367, no. 6481, pp. 979–980, 2020.
- [56] Y. Wang, P. He, and H. Zhou, "Olivine LiFePO4: Development and future," Energy Environ. Sci., vol. 4, no. 3, pp. 805–817, 2011.
- [57] M. Brand et al., "Electrical safety of commercial Li-ion cells based on NMC and NCA technology compared to LFP technology," in Proc. World Electr. Vehicle Symp. Exhib. (EVS), Nov. 2013, pp. 1–9.
- [58] W. Tang, W. C. Tam, L. Yuan, T. Dubaniewicz, R. Thomas, and J. Soles, "Estimation of the critical external heat leading to the failure of lithium-ion batteries," *Appl. Thermal Eng.*, no. 179, pp. 1–10, 2020.
- [59] D. Ansean, M. Gonzalez, V. M. Garcia, J. C. Viera, J. C. Anton, and C. Blanco, "Evaluation of LiFePO<sub>4</sub> batteries for electric vehicle applications," *IEEE Trans. Ind. Appl.*, vol. 51, no. 2, pp. 1855–1863, Jul. 2015.
- [60] D. Li et al., "Degradation mechanisms of C<sub>6</sub>/LiFePO<sub>4</sub> batteries: Experimental analyses of calendar aging," *Electrochim. Acta*, vol. 190, pp. 1124–1133, Feb. 2016.

- [61] X. Han et al., "A review on the key issues of the lithium-ion battery degradation among the whole life cycle," eTransportation, vol. 1, Aug. 2019, Art. no. 100005.
- [62] K. Edström, T. Gustafsson, and J. O. Thomas, "The cathode–electrolyte interface in the Li-ion battery," *Electrochim. Acta*, vol. 50, nos. 2–3, pp. 397–403, 2004.
- [63] R. Hausbrand et al., "Fundamental degradation mechanisms of layered oxide Li-ion battery cathode materials: Methodology, insights and novel approaches," Mater. Sci. Eng., B, vol. 192, pp. 3–25, Feb. 2015.
- [64] K. Amine et al., "Advanced cathode materials for high-power applications," J. Power Sources, vol. 146, nos. 1–2, pp. 111–115, Aug. 2005.
- [65] M. Balasundaram, V. Ramar, C. Yap, L. Li, A. A. O. Tay, and P. Balaya, "Heat loss distribution: Impedance and thermal loss analyses in LiFePO<sub>4</sub>/graphite 18650 electrochemical cell," *J. Power Sources*, vol. 328, pp. 413–421, Oct. 2016.
- [66] D. P. Abraham et al., "Diagnosis of power fade mechanisms in high-power lithium-ion cells," J. Power Sources, vols. 119–121, pp. 511–516, Jun. 2003.
- [67] E. Sarasketa-Zabala, E. Martinez-Laserna, M. Berecibar, I. Gandiaga, L. M. Rodriguez-Martinez, and I. Villarreal, "Realistic lifetime prediction approach for Li-ion batteries," *Appl. Energy*, vol. 162, pp. 839–852, Jan. 2016.
- [68] J. de Hoog et al., "Combined cycling and calendar capacity fade modeling of a Nickel-manganese-cobalt oxide cell with real-life profile validation," Appl. Energy, vol. 200, pp. 47–61, Aug. 2017.
- [69] J. Schmalstieg, S. Käbitz, M. Ecker, and D. U. Sauer, "A holistic aging model for Li(NiMnCo)O<sub>2</sub> based 18650 lithium-ion batteries," *J. Power Sources*, vol. 257, pp. 325–334, Jul. 2014.
- [70] M. Schimpe, M. E. von Kuepach, M. Naumann, H. C. Hesse, K. Smith, and A. Jossen, "Comprehensive modeling of temperature-dependent degradation mechanisms in lithium iron phosphate batteries," *J. Electrochem. Soc.*, vol. 165, no. 2, pp. A181–A193, 2018.
- [71] M. Ecker et al., "Calendar and cycle life study of Li(NiMnCo)O<sub>2</sub>-based 18650 lithium-ion batteries," J. Power Sources, vol. 248, pp. 839–851, Feb. 2014.
- [72] M. Lewerenz and D. U. Sauer, "Evaluation of cyclic aging tests of prismatic automotive Li(NiMnCo)O<sub>2</sub>-graphite cells considering influence of homogeneity and anode overhang," *J. Energy Storage*, vol. 18, pp. 421–434, Aug. 2018.
- [73] M. Lewerenz, J. Münnix, J. Schmalstieg, S. Käbitz, M. Knips, and D. U. Sauer, "Systematic aging of commercial LiFePO<sub>4</sub>|graphite cylindrical cells including a theory explaining rise of capacity during aging," *J. Power Sources*, vol. 345, pp. 254–263, Mar. 2017.
- [74] T. Hüfner, M. Oldenburger, B. Bedürftig, and A. Gruhle, "Lithium flow between active area and overhang of graphite anodes as a function of temperature and overhang geometry," *J. Energy Storage*, vol. 24, Aug. 2019, Art. no. 100790.
- [75] M. Lewerenz, P. Dechent, and D. U. Sauer, "Investigation of capacity recovery during rest period at different states-of-charge after cycle life test for prismatic Li(Ni<sub>1/3</sub>Mn<sub>1/3</sub>Co<sub>1/3</sub>)O<sub>2</sub>-graphite cells," *J. Energy Storage*, vol. 21, pp. 680–690, Feb. 2019.
- [76] M. Lewerenz, G. Fuchs, L. Becker, and D. U. Sauer, "Irreversible calendar aging and quantification of the reversible capacity loss caused by anode overhang," *J. Energy Storage*, vol. 18, pp. 149–159, Aug. 2018.
- [77] T. Bank, J. Feldmann, S. Klamor, S. Bihn, and D. U. Sauer, "Extensive aging analysis of high-power lithium titanate oxide batteries: Impact of the passive electrode effect," *J. Power Sources*, vol. 473, Oct. 2020, Art. no. 228566.
- [78] J. Wilhelm et al., "Cycling capacity recovery effect: A Coulombic efficiency and post-mortem study," J. Power Sources, vol. 365, pp. 327–338, Oct. 2017.
- [79] P. Ramadass, B. Haran, P. M. Gomadam, R. White, and B. N. Popov, "Development of first principles capacity fade model for Li-ion cells," *J. Electrochem. Soc.*, vol. 151, no. 2, p. A196, 2004.
- [80] X. Jin and C. Liu, "Physics-based control-oriented reduced-order degradation model for Li(NiMnCo)O<sub>2</sub>-graphite cell," *Electrochim. Acta*, vol. 312, pp. 188–201, Jul. 2019.
- [81] E. Prada, D. Di Domenico, Y. Creff, J. Bernard, V. Sauvant-Moynot, and F. Huet, "A simplified electrochemical and thermal aging model of LiFePO<sub>4</sub>-graphite Li-ion batteries: Power and capacity fade simulations," J. Electrochem. Soc., vol. 160, no. 4, pp. A616–A628, 2013.
- [82] X. Jin et al., "Physically-based reduced-order capacity loss model for graphite anodes in Li-ion battery cells," J. Power Sources, vol. 342, pp. 750–761, Feb. 2017.

- [83] S. Bashash, S. J. Moura, and H. K. Fathy, "Charge trajectory optimization of plug-in hybrid electric vehicles for energy cost reduction and battery health enhancement," in *Proc. Amer. Control Conf.*, Jun. 2010, pp. 5824–5831.
- [84] J. C. Forman, S. Bashash, J. L. Stein, and H. K. Fathy, "Reduction of an electrochemistry-based Li-ion battery model via quasi-linearization and Padé approximation," *J. Electrochem. Soc.*, vol. 158, no. 2, pp. A93–A101, 2011.
- [85] X. Hu, L. Xu, X. Lin, and M. Pecht, "Battery lifetime prognostics," *Joule*, vol. 4, no. 2, pp. 310–346, Feb. 2020.
- [86] Y. Wang et al., "A comprehensive review of battery modeling and state estimation approaches for advanced battery management systems," Renew. Sustain. Energy Rev., vol. 131, Oct. 2020, Art. no. 110015.
- [87] H. Tian, P. Qin, K. Li, and Z. Zhao, "A review of the state of health for lithium-ion batteries: Research status and suggestions," *J. Cleaner Prod.*, vol. 261, Jul. 2020, Art. no. 120813.
- [88] R. Gu, P. Malysz, H. Yang, and A. Emadi, "On the suitability of electrochemical-based modeling for lithium-ion batteries," *IEEE Trans. Transport. Electrific.*, vol. 2, no. 4, pp. 417–431, Dec. 2016.
- [89] M. Lucu et al., "Data-driven nonparametric Li-ion battery ageing model aiming at learning from real operation data—Part A: Storage operation," J. Energy Storage, vol. 30, Aug. 2020, Art. no. 101409.
- [90] M. Lucu et al., "Data-driven nonparametric Li-ion battery ageing model aiming at learning from real operation data—Part B: Cycling operation," J. Energy Storage, vol. 30, Aug. 2020, Art. no. 101410.
- [91] A. K. Severson, M. P. Attia, N. Jin, N. Perkins, B. Jiang, and Z. Yang, "Data-driven prediction of battery cycle life before capacity degradation," *Nature Energy*, vol. 4, no. 5, pp. 383–391, May 2019.
- [92] B. Saha and K. Goebel. Battery data set. NASA Ames Prognostics Data Repository. Accessed: Sep. 29, 2020. [Online]. Available: http://ti.arc.nasa.gov/project/prognostic-data-repository
- [93] W. He, N. Williard, M. Osterman, and M. Pecht, "Prognostics of lithium-ion batteries based on Dempster–Shafer theory and the Bayesian Monte Carlo method," *J. Power Sources*, vol. 196, no. 23, pp. 10314–10321, Dec. 2011.
- [94] L. Merkle, "Cloud-based battery digital twin middleware using model-based development," in *Proc. ISCSIC*, 2019, pp. 1–7.
- [95] W. Li, M. Rentemeister, J. Badeda, D. Jöst, D. Schulte, and D. U. Sauer, "Digital twin for battery systems: Cloud battery management system with online state-of-charge and state-of-health estimation," *J. Energy Storage*, vol. 30, Aug. 2020, Art. no. 101557.
- [96] I. Baghdadi, O. Briat, J.-Y. Delétage, P. Gyan, and J.-M. Vinassa, "Lithium battery aging model based on Dakin's degradation approach," *J. Power Sources*, vol. 325, pp. 273–285, Sep. 2016.
- [97] I. Bloom et al., "An accelerated calendar and cycle life study of Li-ion cells," J. Power Sources, vol. 101, no. 2, pp. 238–247, 2001.
- [98] J. Wang et al., "Cycle-life model for graphite-LiFePO<sub>4</sub> cells," J. Power Sources, vol. 196, no. 8, pp. 3942–3948, Apr. 2011.
- [99] M. Petit, E. Prada, and V. Sauvant-Moynot, "Development of an empirical aging model for Li-ion batteries and application to assess the impact of vehicle-to-grid strategies on battery lifetime," *Appl. Energy*, vol. 172, pp. 398–407, Jun. 2016.
- [100] G. Suri and S. Onori, "A control-oriented cycle-life model for hybrid electric vehicle lithium-ion batteries," *Energy*, vol. 96, pp. 644–653, Feb. 2016.
- [101] M. Naumann, F. B. Spingler, and A. Jossen, "Analysis and modeling of cycle aging of a commercial LiFePO<sub>4</sub>/graphite cell," *J. Power Sources*, vol. 451, Mar. 2020, Art. no. 227666.
- [102] J. Wang et al., "Degradation of lithium ion batteries employing graphite negatives and nickel-cobalt-manganese oxide + spinel manganese oxide positives: Part 1, aging mechanisms and life estimation," *J. Power Sources*, vol. 269, pp. 937–948, Dec. 2014.
- [103] S. Grolleau et al., "The French SIMCAL research network for modelling of calendar aging for energy storage system in EVs and HEVs-EIS analysis on LFP/C cells," ECS Trans., vol. 45, no. 13, pp. 73–81, Feb. 2013.
- [104] P. Gyan et al., "Experimental assessment of battery cycle life within the SIMSTOCK research program," Oil Gas Sci. Technol.-Revue d'IFP Energies Nouvelles, vol. 68, no. 1, pp. 137–147, 2013.
- [105] M. Naumann, M. Schimpe, P. Keil, H. C. Hesse, and A. Jossen, "Analysis and modeling of calendar aging of a commercial LiFePO<sub>4</sub>/graphite cell," *J. Energy Storage*, vol. 17, pp. 153–169, Jun. 2018.
- [106] E. Sarasketa-Zabala, I. Gandiaga, E. Martinez-Laserna, L. M. Rodriguez-Martinez, and I. Villarreal, "Cycle ageing analysis of a LiFePO<sub>4</sub>/graphite cell with dynamic model validations: Towards realistic lifetime predictions," *J. Power Sources*, vol. 275, pp. 573–587, Feb. 2015.

- [107] E. Sarasketa-Zabala, I. Gandiaga, L. M. Rodriguez-Martinez, and I. Villarreal, "Calendar ageing analysis of a LiFePO<sub>4</sub>/graphite cell with dynamic model validations: Towards realistic lifetime predictions," *J. Power Sources*, vol. 272, pp. 45–57, Dec. 2014.
- [108] D. Werner, S. Paarmann, A. Wiebelt, and T. Wetzel, "Inhomogeneous temperature distribution affecting the cyclic aging of Li-ion cells. Part II: Analysis and correlation," *Batteries*, vol. 6, no. 1, p. 12, 2020.
- [109] D. Werner, S. Paarmann, A. Wiebelt, and T. Wetzel, "Inhomogeneous temperature distribution affecting the cyclic aging of Li-ion cells. Part I: Experimental investigation," *Batteries*, vol. 6, no. 1, p. 13, 2020.
- [110] D. Werner, S. Paarmann, and T. Wetzel, "Calendar aging of Li-ion cells-experimental investigation and empirical correlation," *Batteries*, vol. 7, no. 2, p. 28, 2021.
- [111] F. Todeschini, S. Onori, and G. Rizzoni, "An experimentally validated capacity degradation model for Li-ion batteries in PHEVs applications," *IFAC Proc. Volumes*, vol. 45, no. 20, pp. 456–461, 2012.
- [112] P. Badami et al., "Performance of 26650 Li-ion cells at elevated temperature under simulated PHEV drive cycles," Int. J. Hydrogen Energy, vol. 42, no. 17, pp. 12396–12404, Apr. 2017.
- [113] S. Grolleau et al., "Calendar aging of commercial graphite/LiFePO<sub>4</sub> cell–predicting capacity fade under time dependent storage conditions," J. Power Sources, vol. 255, pp. 450–458, Jun. 2014.
- [114] M. Ecker et al., "Development of a lifetime prediction model for lithium-ion batteries based on extended accelerated aging test data," J. Power Sources, vol. 215, pp. 248–257, Oct. 2012.
- [115] S. Käbitz et al., "Cycle and calendar life study of a graphite|LiNi<sub>1/3</sub>Mn<sub>1/3</sub>Co<sub>1/3</sub>O<sub>2</sub> Li-ion high energy system. Part A: Full cell characterization," J. Power Sources, vol. 239, pp. 572–583, Oct. 2013.
- [116] A. Cordoba-Arenas, S. Onori, Y. Guezennec, and G. Rizzoni, "Capacity and power fade cycle-life model for plug-in hybrid electric vehicle lithium-ion battery cells containing blended spinel and layeredoxide positive electrodes," *J. Power Sources*, vol. 278, pp. 473–483, Mar. 2015.
- [117] A. Chu, A. Allam, A. Cordoba Arenas, G. Rizzoni, and S. Onori, "Stochastic capacity loss and remaining useful life models for lithiumion batteries in plug-in hybrid electric vehicles," *J. Power Sources*, vol. 478, no. 1, 2020, Art. no. 228991.
- [118] C. Zhang, F. Yan, C. Du, J. Kang, and R. Turkson, "Evaluating the degradation mechanism and state of health of LiFePO<sub>4</sub> lithium-ion batteries in real-world plug-in hybrid electric vehicles application for different ageing paths," *Energies*, vol. 10, no. 110, pp. 1–13, 2017.
- [119] K. L. Gering et al., "Investigation of path dependence in commercial lithium-ion cells chosen for plug-in hybrid vehicle duty cycle protocols," J. Power Sources, vol. 196, no. 7, pp. 3395–3403, 2011.
- [120] Z. Chen, J. Lu, B. Liu, N. Zhou, and S. Li, "Optimal energy management of plug-in hybrid electric vehicles concerning the entire lifespan of lithium-ion batteries," *Energies*, vol. 13, no. 10, p. 2543, May 2020.
- [121] Z. Chen, Y. Yang, J. Lu, and R. Xiong, "Research on influence of battery aging on energy management economy for plug-in hybrid electric vehicle," *IEEE Access*, pp. 3117–3121, Oct. 2014.
- [122] L. Tang, G. Rizzoni, and S. Onori, "Energy management strategy for HEVs including battery life optimization," *IEEE Trans. Transport. Electrific.*, vol. 1, no. 3, pp. 211–222, Oct. 2015.
- [123] C. Wang, R. Xiong, H. He, Y. Zhang, and W. Shen, "Comparison of decomposition levels for wavelet transform based energy management in a plug-in hybrid electric vehicle," *J. Cleaner Prod.*, vol. 210, pp. 1085–1097, Feb. 2019.
- [124] C. Wang, R. Yang, and Q. Yu, "Wavelet transform based energy management strategies for plug-in hybrid electric vehicles considering temperature uncertainty," *Appl. Energy*, vol. 256, pp. 1–13, Dec. 2019.
- [125] F. Jin, M. Wang, and C. Hu, "A fuzzy logic based power management strategy for hybrid energy storage system in hybrid electric vehicles considering battery degradation," in *Proc. IEEE Transp. Electrific.* Conf. Expo (ITEC), Jun. 2016, pp. 1–7.
- [126] A. Hoke, A. Brissette, D. Maksimovic, A. Pratt, and K. Smith, "Electric vehicle charge optimization including effects of lithium-ion battery degradation," in *Proc. IEEE Vehicle Power Propuls. Conf.*, Sep. 2011, pp. 1–8.
- [127] J. A. López-Ibarra, H. Gaztañaga, A. Saez-de-Ibarra, and H. Camblong, "Plug-in hybrid electric buses total cost of ownership optimization at fleet level based on battery aging," *Appl. Energy*, vol. 280, Dec. 2020, Art. no. 115887.
- [128] M. Mitch, "Advantages and marine applications of various lithium ion battery chemistries," in *Proc. Marad META Battery Propulsion Conf.*, 2016, pp. 1–18.

- [129] S. J. Moura, J. L. Stein, and H. K. Fathy, "Battery-health conscious power management in plug-in hybrid electric vehicles via electrochemical modeling and stochastic control," *IEEE Trans. Control Syst. Technol.*, vol. 21, no. 3, pp. 679–694, May 2013.
- [130] L. Tang, G. Rizzoni, and A. Cordoba-Arenas, "Battery life extending charging strategy for plug-in hybrid electric vehicles and battery electric vehicles," *IFAC-PapersOnLine*, vol. 49, no. 11, pp. 70–76, 2016.
- [131] J. Du et al., "Battery degradation minimization oriented energy management strategy for plug-in hybrid electric bus with multi-energy storage system," Energy, vol. 165, no. 1, pp. 153–163, Dec. 2018.
- [132] Z. Song et al., "Multi-objective optimization of a semi-active battery/supercapacitor energy storage system for electric vehicles," Appl. Energy, vol. 135, pp. 212–224, Dec. 2014.
- [133] J. Hu, Z. Hu, X. Niu, and Q. Bai, "Research on energy management strategy considering battery life for plug-in hybrid electric vehicle," *Adv. Mech. Eng.*, vol. 10, no. 9, pp. 1–12, Sep. 2018.
- [134] Y. Wang, X. Jiao, Z. Sun, and P. Li, "Energy management strategy in consideration of battery health for PHEV via stochastic control and particle swarm optimization algorithm," *Energies*, vol. 10, no. 11, p. 1894, 2017.
- [135] S. Onori, P. Spagnol, V. Marano, Y. Guezennec, and G. Rizzoni, "A new life estimation method for lithium-ion batteries in plug-in hybrid electric vehicles applications," *J. Power Electron.*, vol. 4, no. 3, pp. 302–319, 2012.
- [136] X. Jiao, T. Shen, and M. Sasaki, "Policy iteration algorithm-based energy management with battery lifetime consideration for commute hybrid electric vehicles," in *Proc. EVTeC APE Japan*, 2014, pp. 22–24.
- [137] M. Sasaki and T. Shen, "EV bus system control strategy design with consideration of battery lifetime model," in *Proc. 10th Int. Power Energy Conf. (IPEC)*, Nov. 2012, pp. 213–217.
- [138] S. Bashash, S. J. Moura, J. C. Forman, and H. K. Fathy, "Plug-in hybrid electric vehicle charge pattern optimization for energy cost and battery longevity," *J. Power Sources*, vol. 196, no. 1, pp. 541–549, Jan. 2011.
- [139] T. Miro-Padovani, M. Debert, G. Colin, and Y. Chamaillard, "Optimal energy management strategy including battery health through thermal management for hybrid vehicles," *IFAC Proc. Volumes*, vol. 46, no. 21, pp. 384–389, 2013.
- [140] Y. Cai, M. G. Ouyang, and F. Yang, "Impact of power split configurations on fuel consumption and battery degradation in plug-in hybrid electric city buses," *Appl. Energy*, vol. 188, pp. 257–269, Feb. 2017.
- [141] Z. Song, H. Hofmann, J. Li, X. Han, X. Zhang, and M. Ouyang, "A comparison study of different semi-active hybrid energy storage system topologies for electric vehicles," *J. Power Sources*, vol. 274, pp. 400–411, Jan. 2015.
- [142] Z. Song, H. Hofmann, J. Li, X. Han, and M. Ouyang, "Optimization for a hybrid energy storage system in electric vehicles using dynamic programing approach," *Appl. Energy*, vol. 139, pp. 151–162, Feb. 2015.
- [143] Y. Liang and S. Makam, "PHEV hybrid vehicle system efficiency and battery aging optimization using A-ECMS based algorithms," SAE Int., pp. 1–9, Apr. 2020.
- [144] A. Mamun, I. Narayanan, D. Wang, A. Sivasubramaniam, and H. K. Fathy, "Multi-objective optimization of demand response in a datacenter with lithium-ion battery storage," *J. Energy Storage*, vol. 7, pp. 258–269, Aug. 2016.
- [145] L. Han, X. Jiao, and Z. Zhang, "Recurrent neural network-based adaptive energy management control strategy of plug-in hybrid electric vehicles considering battery aging," *Energies*, vol. 13, no. 1, p. 202, Jan. 2020.
- [146] L. Serrao, S. Onori, A. Sciarretta, Y. Guezennec, and G. Rizzoni, "Optimal energy management of hybrid electric vehicles including battery aging," in *Proc. Amer. Control Conf.*, Jun. 2011, pp. 2125–2130.
- [147] S. Zhang, X. Hu, S. Xie, Z. Song, L. Hu, and C. Hou, "Adaptively coordinated optimization of battery aging and energy management in plug-in hybrid electric buses," *Appl. Energy*, vol. 256, Dec. 2019, Art. no. 113891.
- [148] N. Sockeel, J. Shi, M. Shahverdi, and M. Mazzola, "Sensitivity analysis of the vehicle model mass for model predictive control based power management system of a plug-in hybrid electric vehicle," in *Proc. IEEE Transp. Electrific. Conf. Expo (ITEC)*, Jun. 2018, pp. 767–772.
- [149] N. Sockeel, J. Shi, M. Shahverdi, and M. Mazzola, "Sensitivity analysis of the battery model for model predictive control: Implementable to a plug-in hybrid electric vehicle," World Electr. Veh. J., vol. 9, no. 45, pp. 1–18, 2018.

- [150] N. Sockeel, J. Shi, M. Shahverdi, and M. Mazzola, "Pareto front analysis of the objective function in model predictive control based power management system of a plug-in hybrid electric vehicle," in *Proc. IEEE Transp. Electrific. Conf. Expo (ITEC)*, Jun. 2018, pp. 971–976.
- [151] H.-Q. Guo, C.-Z. Liu, J.-W. Yong, X.-Q. Cheng, and F. Muhammad, "Model predictive iterative learning control for energy management of plug-in hybrid electric vehicle," *IEEE Access*, vol. 7, pp. 71323–71334, 2019.
- [152] X. Zhang, L. Guo, N. Guo, Y. Zou, and G. Du, "Bi-level energy management of plug-in hybrid electric vehicles for fuel economy and battery lifetime with intelligent state-of-charge reference," *J. Power Sources*, vol. 481, Jan. 2021, Art. no. 228798.
- [153] N. Guo, X. Zhang, Y. Zou, L. Guo, and G. Du, "Real-time predictive energy management of plug-in hybrid electric vehicles for coordination of fuel economy and battery degradation," *Energy*, vol. 214, Jan. 2021, Art. no. 119070.
- [154] E. Taherzadeh, H. Radmanesh, and A. Mehrizi-Sani, "A comprehensive study of the parameters impacting the fuel economy of plug-in hybrid electric vehicles," *IEEE Trans. Intell. Vehicles*, vol. 5, no. 4, pp. 596–615, Dec. 2020.
- [155] Z. Song, X. Zhang, J. Li, H. Hofmann, M. Ouyang, and J. Du, "Component sizing optimization of plug-in hybrid electric vehicles with the hybrid energy storage system," *Energy*, vol. 144, pp. 393–403, Feb. 2018.



**Tobias Frambach** received the M.Sc. degree in automotive engineering and transport from RWTH Aachen University, Aachen, Germany, in 2019, where he is currently pursuing the Ph.D. degree with the Institute for Power Electronics and Electrical Drives in cooperation with Robert Bosch GmbH, Schwieberdingen, Germany.

His research focuses on powertrain simulation and optimization of hybrid electric vehicles for passenger cars. Next to generating electrical and thermal battery simulation models, he additionally investigates

the aging behavior of batteries in lab experiments and the consequential impact on powertrain sizing.



Ralf Liedtke received the Ph.D. degree in materials science for electronics from RWTH Aachen University, Aachen, Germany, in 2003.

He started his work at corporate research at Robert Bosch GmbH, Schwieberdingen, Germany, with a special focus on the development of high-energy lithium-ion cells as a Project Leader. From 2017 to 2018, he was occupied at Robert Bosch Battery Systems GmbH, Stuttgart, Germany, as a Group Leader for cell chemistry engineering. Since 2018, he has been continuing his work in the Systems

Engineering Powertrain Department for Hybrid Electric Vehicles, Robert Bosch GmbH, as a Group Leader. His current area of work includes the field of battery system engineering and simulation for new powertrain architectures.



**Philipp Dechent** is currently pursuing the Ph.D. degree with the Dirk Uwe Sauers Lab of Electrochemical Energy Conversion and Storage Systems, RWTH Aachen University, Aachen, Germany.

His work focuses on battery testing and effects as reversibly capacity loss and the influence of cell-to-cell variation on lifetime. He is conducting large-scale aging experiments for sufficient input data for Monte Carlo aging simulations with initial variation and aging rate differences. He is also the Lead Engineer with the Center of Ageing, Reliability

and Lifetime Prediction, Aachen, with a start of operation in early 2022.



Dirk Uwe Sauer has been working on batteries and renewable energy systems since 1992 and became a Professor of electrochemical energy conversion and storage systems at RWTH Aachen University, Aachen, Germany, in 2003. His focus is on researching processes, diagnostic systems, and test procedures to predict the durability of battery systems. In addition, he researches practical types of battery applications especially for mobility with application in the field of passenger cars and in public transport. He has a holistic view of batteries, including

postmortem analysis, aging and lifetime prediction, modeling and diagnostics, impedance spectroscopy and impedance-based modeling, and energy system analysis including sector coupling.

Prof. Sauer is also the Chair of the Board of Directors of the Interdisciplinary Policy Advisory Project of the National Science Academies "Energy Systems of the Future" on all aspects of the "Energiewende." He is also the Editor-in-Chief of the *Journal of Energy Storage*.



**Egbert Figgemeier** received the Ph.D. degree in chemistry from the University of Paderborn, Paderborn, Germany, in 1998.

This was followed by academic research at University College Dublin, Dublin, Ireland, the University of Basel, Basel, Switzerland, and the University of Uppsala, Uppsala, Sweden. In 2007, he joined Bayer Technology Services, Leverkusen, Germany, heading the Materials and Corrosion Lab and the development of materials for battery applications. Since 2012, he has been an Application Develop-

ment Engineer for battery materials with 3M Deutschland, Neuss, Germany, responsible for technical support of customers in Germany and Europe. His focus in battery materials was negative electrode materials of the next generation and assembly materials for battery backs and modules. Since 2016, he has been the Group Leader with the Helmholtz Institute Münster, Forschungszentrum Jülich (Section Aachen), Münster, Germany. He also holds the Chair for "Ageing and Reliability of Batteries" at RWTH Aachen University, Aachen, Germany. His current research activities span from fundamental aging mechanisms in lithium-ion and lithium metal batteries to the development of electrolyte additives and prelithiation technologies.